

2014

Immobilizing Mutation in an Unconventional Myosin15a Affects not only the Structure of Mechanosensory Stereocilia in the Inner Ear Hair Cells but also their Ionic Conductances

Diana Syam

University of Kentucky, diana.syam@uky.edu

[Right click to open a feedback form in a new tab to let us know how this document benefits you.](#)

Recommended Citation

Syam, Diana, "Immobilizing Mutation in an Unconventional Myosin15a Affects not only the Structure of Mechanosensory Stereocilia in the Inner Ear Hair Cells but also their Ionic Conductances" (2014). *Theses and Dissertations--Medical Sciences*. 2.

https://uknowledge.uky.edu/medsci_etds/2

This Master's Thesis is brought to you for free and open access by the Medical Sciences at UKnowledge. It has been accepted for inclusion in Theses and Dissertations--Medical Sciences by an authorized administrator of UKnowledge. For more information, please contact UKnowledge@lsv.uky.edu.

STUDENT AGREEMENT:

I represent that my thesis or dissertation and abstract are my original work. Proper attribution has been given to all outside sources. I understand that I am solely responsible for obtaining any needed copyright permissions. I have obtained needed written permission statement(s) from the owner(s) of each third-party copyrighted matter to be included in my work, allowing electronic distribution (if such use is not permitted by the fair use doctrine) which will be submitted to UKnowledge as Additional File.

I hereby grant to The University of Kentucky and its agents the irrevocable, non-exclusive, and royalty-free license to archive and make accessible my work in whole or in part in all forms of media, now or hereafter known. I agree that the document mentioned above may be made available immediately for worldwide access unless an embargo applies.

I retain all other ownership rights to the copyright of my work. I also retain the right to use in future works (such as articles or books) all or part of my work. I understand that I am free to register the copyright to my work.

REVIEW, APPROVAL AND ACCEPTANCE

The document mentioned above has been reviewed and accepted by the student's advisor, on behalf of the advisory committee, and by the Director of Graduate Studies (DGS), on behalf of the program; we verify that this is the final, approved version of the student's thesis including all changes required by the advisory committee. The undersigned agree to abide by the statements above.

Diana Syam, Student

Dr. Gregory I. Frolenkov, Major Professor

Dr. Joe E. Springer, Director of Graduate Studies

IMMOBILIZING MUTATION IN AN UNCONVENTIONAL MYOSIN15A
AFFECTS NOT ONLY THE STRUCTURE OF MECHANOSENSORY
STEREOCILIA IN THE INNER EAR HAIR CELLS BUT ALSO THEIR
IONIC CONDUCTANCES

THESIS

A thesis submitted in partial fulfillment of the
requirements for the degree of Master of Science in the
College Medicine at the University of Kentucky

By

Diana F. Syam

Cluj-Napoca, Romania

Director: Dr. Gregory I. Frolenkov

Associate Professor at the Physiology Department

Lexington, Kentucky

2014

Copyright © Diana F. Syam 2013

ABSTRACT OF THESIS

IMMOBILIZING MUTATION IN AN UNCONVENTIONAL MYOSIN15A AFFECTS NOT ONLY THE STRUCTURE OF MECHANOSENSORY STEREOCILIA IN THE INNER EAR HAIR CELLS BUT ALSO THEIR IONIC CONDUCTANCE

In the inner and outer hair cells (OHCs) of the inner ear, an unconventional myosin 15a localizes at the tips of mechanosensory stereocilia and plays an important role in forming and maintaining their normal structure. A missense mutation makes the motor domain of myosin 15a dysfunctional and is responsible for the congenital deafness DFNB3 in humans and deafness and vestibular defects in *Shaker-2* (*Sh2*) mouse model. All hair cells of homozygous *Shaker-2* mice (*Myo15^{sh2/sh2}*) have abnormally short stereocilia, but, only stereocilia of *Myo15^{sh2/sh2}* OHCs start to degenerate after the first few days of postnatal development and lose filamentous tip links between stereocilia that are crucial for mechanotransduction. The exact mechanisms of this degeneration are unknown even though they may underlie DFNB3 deafness in humans. We hypothesize that structural abnormalities in *Myo15^{sh2/sh2}* OHCs may alter the mechanical forces applied to the mechano-electrical transduction (MET) channels resulting in abnormal ionic homeostasis, which may lead to eventual degeneration of *Myo15^{sh2/sh2}* OHCs. Therefore, we investigated the ionic conductances and integrity of mechanotransduction apparatus in *Myo15^{sh2/sh2}* OHCs. Surprisingly, we found that myosin 15a-deficiency is associated not only with structural abnormalities of OHC stereocilia but also with alterations of voltage-gated ion conductances.

KEYWORDS: Organ of Corti, Outer Hair Cells, Myosin15a,
Shaker-2 Mice, Patch Clamp.

Diana F. Syam

Apr. 8th, 2014

IMMOBILIZING MUTATION IN AN UNCONVENTIONAL MYOSIN15A
AFFECTS NOT ONLY THE STRUCTURE OF MECHANOSENSORY
STEREOCILIA IN THE INNER EAR HAIR CELLS BUT ALSO THEIR
IONIC CONDUCTANCES

By

Diana F. Syam

Dr. Gregory I. Frolenkov
Advisor

Dr. Joe E. Springer
Director of Graduate Studies

Apr. 8th, 2014

For my mom; the center of my universe.

Acknowledgements

I would like to thank my advisor, Dr. Gregory I. Frolenkov, for teaching me to think critically in class, in the lab and life in general. His continuous guidance and patience are very much appreciated. I also would like to extend my thanks to my committee members; Dr. Karyn Esser, Dr. Lu-Yuan Lee and Dr. Brian Delisle. Their input and feedback are extremely valued. I also would like to acknowledge NIH for their support and funding.

My gratitude to my lab colleagues, specifically A. Catalina Vélez-Ortega and Ghanshyam Sinha for teaching me all the techniques I used in this work. Stephanie Edelmann, Mike Grossheim and Shadan Hadi; your input and feedback during our lab meetings were very helpful.

Infinite love, appreciation and thanks go to my family; my parents, grandparents (Mihail and Elena) and little brothers. Your support and encouragement helped me throughout the journey and I am forever grateful. A special thank you to my mom, who never acknowledged the limitations I put on myself and always pushed me forward. And finally, I would like to thank my husband, Samir Rawashdeh, my rock, who always believed in me and whose love, advice and constructive criticism helped me through all the rough times during my studies and life in general.

Table of Contents

ACKNOWLEDGEMENTS	III
LIST OF TABLES	VI
LIST OF FIGURES.....	VII
CHAPTER 1 WORK OVERVIEW.....	1
CHAPTER 2 INTRODUCTION	3
CHAPTER 3 BACKGROUND.....	6
3.1 DEAFNESS PREVALENCE AND MANAGEMENT IN THE USA.....	6
3.2 ANATOMY AND CELL BIOLOGY OF THE MAMMALIAN INNER EAR.....	7
3.2.1 <i>The Cochlea</i>	9
3.2.2 <i>The Organ of Corti</i>	11
3.3 MYOSIN PROTEINS	14
3.3.1 <i>Myosin 15a</i>	15
3.3.2 <i>Myosin 15a interaction with Whirlin and other proteins</i>	16
3.4 MECHANOTRANSDUCTION	18
3.5 MECHANOELECTROTRANSDUCTION CHANNEL BLOCKERS	20
3.5.1 <i>Amiloride</i>	20
3.5.2 <i>Dihydrostreptomycin</i>	20
3.6 GENETICS OF DEAFNESS	22
3.6.1 <i>Non-syndromic congenital sensorineural deafness</i>	22
3.6.2 <i>DFNB3 deafness</i>	23
3.7 SHAKER2 MOUSE MODEL	24
3.8 THESIS OBJECTIVE	25
CHAPTER 4 MATERIAL AND METHODS.....	26
4.1 COCHLEA DISSECTION	26
4.2 MOUSE GENOTYPING	28
4.3 COUNTING STEREOCILIA LINKS	30
4.4 FLUORESCENT IMAGING WITH FM1-43FX.....	30
4.5 WHOLE-CELL PATCH CLAMP.....	32
CHAPTER 5 RESULTS AND DISCUSSION.....	35
5.1 STEREOCILIA LINKS RAPIDLY DETERIORATE IN <i>MYO15^{SH2/SH2}</i> MICE	35
5.2 FM1-43FX UPTAKE IN <i>MYO15^{SH2/SH2}</i> OHCS INDICATE THE PRESENCE OF CONSTITUTIVELY OPEN NON-SELECTIVE CATION CHANNELS	38
5.3 <i>MYO15^{SH2/SH2}</i> MUTATION RESULTS IN AN INCREASED OUTWARD CURRENT IN OHCS	

AND A MORE NEGATIVE INTRACELLULAR POTENTIAL	39
5.4 BLOCKING OF MET CURRENT REVEALED THE “STANDING CURRENT” IN <i>MYO15</i> ^{SH2/SH2} OHCS AND POTENTIAL CA ²⁺ -DEPENDENT MODULATION OF THE VOLTAGE-GATED OUTWARD CURRENT	42
CHAPTER 6 SUMMARY	45
CHAPTER 7 CONCLUSION	47
APPENDIX A	49
REFERENCES	50
VITA	60

List of Tables

Table 1-1: Summary of differences between OHCs and IHCs.....	13
--	----

List of Figures

Figure 3.2-1: Gross anatomy of the outer, middle and inner ear.	7
Figure 3.2-2: Cross section in the cochlea.	9
Figure 3.2-3: The Organ of Corti.	11
Figure 3.3-1: Structure of Myosin15a.	15
Figure 3.3-2: Myosin15a is located at the tips of hair cell stereocilia.	16
Figure 3.3-3: The interaction between domains of Myosin15a, Whirlin and Eps8.	17
Figure 3.4-1: MET channel is gated directly or indirectly by a tensioned tip link.	19
Figure 3.5-1: MET channel blocked by blockers in a “bottle cork” mechanism.	21
Figure 3.7-1: Degeneration of stereocilia with age in <i>Myo15^{sh2/sh2}</i>	24
Figure 4.1-1: Culturing the Organ of Corti explant.	27
Figure 4.2-1: The difference between <i>Myo15^{sh2/sh2}</i> (top) and <i>Myo15^{+sh2}</i> (bottom) IHCs.	29
Figure 4.3-1: Counting links and stereocilia in a <i>Myo15^{sh2/sh2}</i> OHC.	30
Figure 4.4-1: Labeling hair cells with FM1-43FX.	31
Figure 4.5-1: Illustration showing set up and procedure for whole cell patch-clamp recordings.	33
Figure 5.1-1: Degeneration of stereocilia in <i>Myo15^{sh2/sh2}</i> with age.	36
Figure 5.1-2: Progressive loss of stereocilia links in postnatal <i>Myo15^{sh2/sh2}</i> outer hair cells with age.	37
Figure 5.2-1: FM1-43FX uptake in <i>Myo15^{sh2/sh2}</i> OHCs.	38
Figure 5.3-1: Ionic currents in <i>Myo15^{+sh2}</i> and <i>Myo15^{sh2/sh2}</i> OHCs.	41
Figure 5.4-1: Effect of drugs blocking MET current on OHC ionic conductance.	43
Figure 5.4-2: Reversal potential (V_{rev}) in <i>Myo15^{+sh2}</i> and <i>Myo15^{sh2/sh2}</i> OHCs	44
Figure 7-1: “Standing current” through partially open MET channels.	48

Chapter 1 Work Overview

In the inner ear, hair cells are organized in one row of inner and three rows of outer hair cells (OHCs). *Myo15* encodes unconventional myosin 15a, a motor protein that localizes at the tips of mechanosensory stereocilia in the hair cells and plays an important role in forming and maintaining their normal structure. The molecular identity of channels responsible for mechano-electrical transduction (MET) in the mammalian hair cells is yet unknown, but number of evidence indicate that these channels are co-localized with myosin 15a at the tips of stereocilia. A missense mutation makes the motor domain of myosin 15a dysfunctional and is responsible for the congenital deafness, DFNB3 in humans and deafness and vestibular defects in the mouse model, *Shaker-2* (*Sh2*) mice. Both inner and outer hair cells of homozygous *Shaker-2* mice (*Myo15^{sh2/sh2}*) have abnormally short stereocilia, but after the first few days of postnatal development, only *Myo15^{sh2/sh2}* OHCs start to degenerate and lose interconnecting filamentous links that are crucial for mechanotransduction. The exact mechanisms of this degeneration are unknown even though they may underlie DFNB3 deafness in humans. Transfection of these cells with wild type *Myo15a* rescues abnormal hair bundle morphology. We hypothesize that structural abnormalities in *Myo15^{sh2/sh2}* hair cells may result in altering mechanical forces applied to the MET channels. Abnormal ionic homeostasis may lead to eventual degeneration of *Myo15^{sh2/sh2}* hair cells. Therefore, we investigated the ionic conductance and the integrity of mechanotransduction in young postnatal *Myo15^{sh2/sh2}* OHCs. Examination of the scanning electron microscopy (SEM) images of *Myo15^{sh2/sh2}* OHCs revealed dramatic degeneration of stereocilia links after postnatal day 3 (P3). Despite this degeneration, we observed fast intracellular accumulation of FM1-43FX, a small cationic dye that is known to permeate through the MET channels, indicating that the MET channels are still open at rest in *Myo15^{sh2/sh2}* OHCs. A standing current that continuously flows into the cell through MET channels may result in a continuous influx of calcium leading to cell degeneration. Indeed, whole cell patch-clamp recordings revealed significant MET channel-dependent component of the ionic current in *Myo15^{sh2/sh2}* OHCs that was blocked by either dihydropyridine (DHP) or Amiloride, known blockers of the MET channels. Surprisingly, patch-clamp experiments also revealed an increased voltage-gated outward conductance and a more negative intracellular potential in *Myo15^{sh2/sh2}* OHCs as compared to control normal-functioning OHCs of *Myo15^{+/sh2}* littermates. This conductance was further increased upon blocking of the MET channels. We speculated that

Myo15^{sh2/sh2} OHCs with abnormally short stereocilia have to compensate for a decreased Ca^{2+} extrusion via stereociliar PMCA pumps. This compensation may include: 1) expression of additional voltage-gated K^{+} channels to maintain intracellular potential; and 2) development of Ca^{2+} -dependent modulation of K^{+} -conductance. To the best of our knowledge, it is the first time that myosin 15a-deficiency has been associated with alterations of voltage-gated ion conductance.

Chapter 2 Introduction

Deafness is a common disability in people of all ages. It is estimated that around 17% of American adults report some degree of hearing loss and about two to three out of every 1,000 children are born deaf or hard-of-hearing. Also, nine out of every ten children who are born deaf are born to hearing parents (1). Unfortunately, in vast majority of the cases, the hearing loss cannot be restored and can only be partially alleviated by cochlear implants and hearing aids.

Hearing loss can be classified into different nomenclature depending on the cause (genetic, acquired due to loud noise, etc.) or region (middle ear, sensorial damage, neuronal damage). One classification is that deafness can be syndromic (i.e. occurs as a clinical symptom for certain genetic diseases) or non-syndromic where it is not associated with any syndrome but is the result of either a dominant, recessive, X-linked or mitochondrial mutations that cause changes in middle or inner ear or the auditory nerve. For example, one of many autosomal recessive non-syndromic congenital types of deafness, DFNB3, is investigated in this thesis and is caused by a recessive mutation. It was first identified in families from Bengkala, Bali in Indonesia (2). DFNB3 is associated with mutation in *Myo15* gene that encodes an unconventional Myosin15 (2).

In the cochlea, mechanosensory cells in the Organ of Corti form one row of inner hair cells (IHCs) and three rows of outer hair cells (OHCs). The apex of the hair cells contains specialized mechanosensory microvilli-like protrusions known as stereocilia. In wild type mammalian hair cells, the stereocilia are arranged into three rows forming characteristic staircase architecture of the hair bundle that may have an important role in its mechanosensitivity. Deflection of stereocilia stretches the tip link filaments that connect the tips of the shorter stereocilia to the adjacent taller stereocilia and are thought to mechanically gate mechanotransduction (MET) channel (Figure 3.4-1: MET channel is gated directly or indirectly by a tensioned tip link and is co-localized at the tips of stereocilia with Myosin15a.). Flow of current into the hair cell through the channel depolarizes the

cells, which results in synaptic transmission to the auditor nerve that convey sound information to the auditory centers in the brain.

Stereocilia are supported by a core of parallel F-actin filaments that interact with numerous actin-binding proteins like; myosin Ic, myosin VIIa, myosin IIIa, and the unconventional myosin-15a (encoded by *Myo15a*). Myosin 15a is present at tips of stereocilia in wild type OHCs and IHCs (3) and is important for maintaining the normal structure of stereocilia. Myosin 15a interacts with a scaffold protein, whirlin, and carries it to the tips of stereocilia, in addition to actin-bundling protein Eps8. DFNB3 is caused by a missense mutation that renders Myosin15a protein dysfunctional and so it is missing from the stereocilia of mutant cells. (3)

Shaker-2 (*Myo15^{sh2/sh2}*) is a mouse model for DFNB3 (2) (4) . The phenotype of *Myo15^{sh2/sh2}* hair cells is well defined. Young postnatal *Myo15^{sh2/sh2}* mice have hair cells with abnormally short stereocilia that still have their tip links and so are mechanosensitive (5). OHCs, but not IHCs, maintain stair-case morphology of the hair bundle. These mice have vestibular defects displayed as head tossing, running in a circular manner, and are profoundly deaf, as indicated by the lack of auditory brain stem responses (4; 5). Older *Myo15^{sh2/sh2}* mice lose their tip links and their OHC, but not IHC, stereocilia degenerates (5). The *Shaker-2* missense mutation also affects the actin cytoskeleton of the cell. Scanning laser confocal microscopy observations show that the actin filaments grow and continue to extend to the base of the cell and beyond the basal membrane up to 50 μm (6).

In young *Myo15^{sh2/sh2}*, the MET channel is still present and it is functional. With age, as the stereocilia degenerate, it is not clear what happens to the channel. The MET channel is a voltage-independent (7; 8), non-selective cation channel that is highly permeable to Ca^{2+} . (9; 10; 8; 11; 12). The exact molecular identity of the MET channel is not known. Pharmacological testing of the pore size was done to characterize the MET channel's

molecular identity but it didn't result in any definitive result. The MET channel is thought to be co-localized with Myosin 15a at the tips of stereocilia (13).

In OHCs of *Myo15^{sh2/sh2}*, the degenerating stereocilia withstand structural abnormalities due to the dysfunctional Myosin15a. We hypothesize that it may cause redistribution of mechanical forces to the MET channels and keep them open, resulting in a standing current that continuously flows into the hair cell. The continuous influx of Ca^{2+} may result in disassembly and degeneration of stereocilia and other cytoskeletal elements of the hair cell.

The original goal of this study was to investigate the existence of a potential “standing current” in *Myo15^{sh2/sh2}* OHCs with different methods. First, investigation of fast uptake of FM1-43FX dye into the *Myo15^{sh2/sh2}* OHCs was planned to reveal the MET channels that are partially open at rest. Next, whole cell patch-clamp recording were planned to determine the resting ionic conductance in *Myo15^{sh2/sh2}* and *Myo15^{+/-sh2}* OHCs that are sensitive to either Dihydrostreptomycin (DHS) or Amiloride (Amil), the known blockers of MET channels. Finally, we also planned to count stereocilia links in degenerating *Myo15^{sh2/sh2}* OHCs using scanning electron microscopy (SEM) images.

The following chapters will provide background to relevant concepts and motivation to the work on this thesis. Chapter one contains an extended abstract that overviews the work done in the thesis. Chapter two provides a brief introduction. In chapter three, the prevalence of deafness in the USA, inner ear's anatomy, physiology, hair cell biology and genetics of deafness will be briefly reviewed. Chapter four will describe the methods and techniques used to get the results by providing a thorough summary about stereocilia link count, FM1-43FX loading and whole cell patch-clamp. Chapter five will discuss the results obtained by the described methods. Summary of the thesis is in chapter six and chapter seven will contain conclusion and hypothesized model to explain the obtained results.

Chapter 3 Background

3.1 Deafness prevalence and management in the USA

Hearing is one of the five basic senses that have evolved over time and has very important role in communication and alertness to surrounding environment which, in turn, are important for survival. Not all species can hear at the same range of frequency. In fact, the amplitude and frequency audible for species who mainly communicate using sounds depends on the range of pitches used by the species' individuals. In humans, for example, the audible frequencies range between 20 Hz and 20 kHz.

The National Institute on Deafness and other Communication Disorders (NIDCD) estimated that 2-3 per 1000 children are born with some type of deafness and of those children, nine out of ten are born to hearing parents (14). The consequences of being profoundly deaf affect not only the child's social and academic life but also the parents and the family who will find it difficult to speak, teach and communicate with the child which can further alienate the deaf child. Therefore, it is essential that deafness is diagnosed early so that it can be addressed by parents to help the affected child.

Deafness is often caused either by damaged hair cells which detect or amplify sound waves or damaged auditory nerve that relays electrical signals from the hair cells to the brain. There are only few available methods that may, to certain extent, alleviate the deafness. One of which is the technology of Hearing aids which has advanced greatly and many types are manufactured and can be adjusted depending on the user's needs. On the other hand, in the case of profound deafness, the hair cells are completely damaged and cochlear implants are used to bypass the hair cells and stimulate the auditory nerve directly. Recent experiments, however, attempt to regenerate damaged hair cells and the auditory nerve, which normally are terminally differentiated and do not regenerate. Using Human embryonic stem cells (hESCs),

hair-cell-like cells and auditory neurons were obtained in vitro and when transplanted into a model of auditory neuropathy, the auditory threshold of the model improved significantly (15). However, these experimental approaches are yet very far from clinical practice.

3.2 Anatomy and Cell Biology of the Mammalian Inner Ear

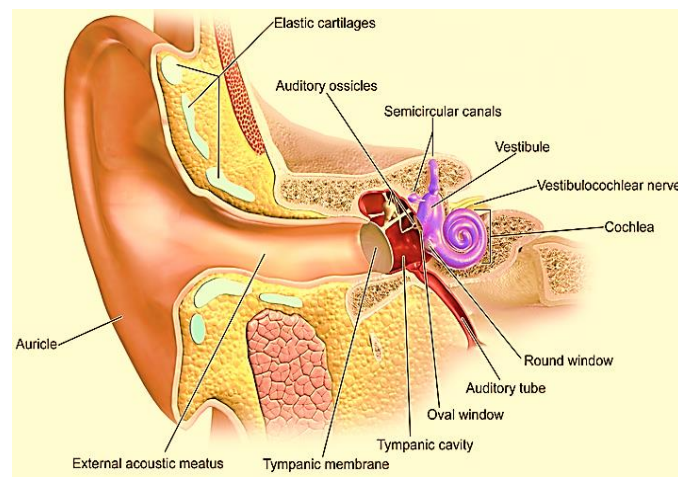


Figure 3.2-1: Gross anatomy of the outer, middle and inner ear.

Image credit: Wikimedia Commons (16)

The ear is an organ with two functions; detecting sound waves of specific frequency range and also detection of head position and movement. For the purpose of this thesis, only the hearing function will be explained.

In order to hear a sound wave that is in the audible frequency range, it must be conducted and sensed by those sensory cells, amplified and transmitted to the auditory region in the brain.

Figure 3.2-1 shows the gross anatomy of the auditory system which, in general, has three components; the outer, middle and inner ear. A brief anatomical and physiological description about each part will be presented next, focusing mainly on the inner ear.

Outer ear: It includes the pinna, ear canal and the ear drum. The pinna functions as a filter by providing a directional guide for sound localization as well as a funnel that collects surrounding sound waves and directs them into the ear canal where eventually they vibrate the eardrum. This part of the ear amplifies sound waves that are between 1.5 kHz and 7 kHz by 10-15dB (17).

Middle ear: Consists of the ossicles, which are the smallest bones in the body; malleus, incus and stapes. Sound waves are transmitted from the ear drum through the ossicles to the oval window which separates the inner ear from the middle ear. The middle ear functions as a mediator that overcomes the acoustic impedance¹ that results if sound-waves crossed directly from the air-filled outer ear into fluid-filled inner ear.

Inner ear: Inner ear has developed from the otic placode. It is located in the temporal bone and is identified by the bony labyrinth that consists of two systems: the cochlea, which is the sound receptor system and the main focus of this thesis, and the vestibule and semi-circular canals that make the balance system.

¹ Acoustic impedance: Pressure generated by sound waves at a given frequency in a particular medium.

3.2.1 The Cochlea

The cochlea is located in the bony labyrinth of the inner ear. From the outside, the cochlea is a bony, snail-shaped shell that coils in 2.5 turns from the base to apex. On the inside, however, it is divided via the cochlear duct and the basilar membrane forming three partitions or scaleae; scala vestibuli, scala media and scala tympani that are filled with either perilymph or endolymph fluid (Figure 3.2-2: Cross section in the cochlea showing the three portions of the cochlea, scaleae and the spiral ganglion of the auditory nerve.). Each of these partitions and fluids has an important function in facilitating the sense of hearing either in a mechanical or chemical manner. The organ of Corti (to be explained in more details in the following section) is located between the scala media and scala tympani.

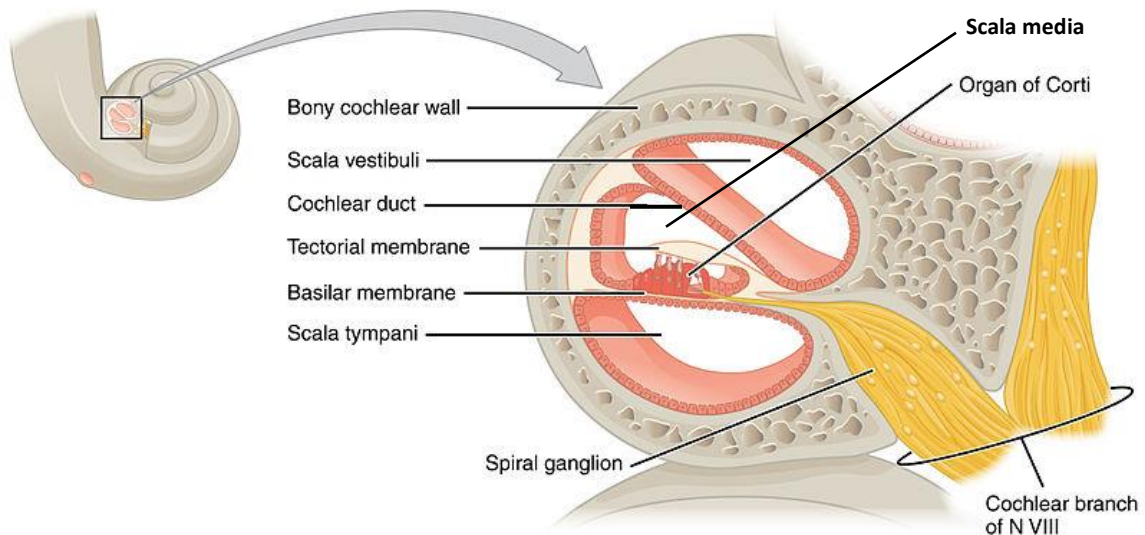


Figure 3.2-2: Cross section in the cochlea showing the three portions of the cochlea, scaleae and the spiral ganglion of the auditory nerve.

Image credit: Wikimedia Commons (18)

There are two types of cochlear fluids:

- **Perilymph:** fills both scala vestibule and scala tympani and bathes the body of hair cells. Perilymph has an ionic composition similar to extracellular fluid; ~

140mM Na^+ , ~ 5mM K^+ and 1.2mM Ca^{2+} (19).

- **Endolymph:** fills scala media and immerses the apical part of the hair cell and its stereocilia. It has a distinctive ionic composition that is not found anywhere else in the body; ~150mM K^+ , ~1mM Na^+ and very low Ca^{2+} (~ 20uM), and a positive potential (+80mV) (19).

The distinctive composition of the cochlear fluid saves the cochlea from spending energy in regulating the flow of K^+ into and out of the hair cell. The high concentration of K^+ in the endolymph results in flow of K^+ ions into the hair cell when its non-selective mechanotransduction channels are open. K^+ ions also flow out of the cell body into perilymph because of the difference in its concentration between the cell body and the perilymph.

3.2.2 The Organ of Corti

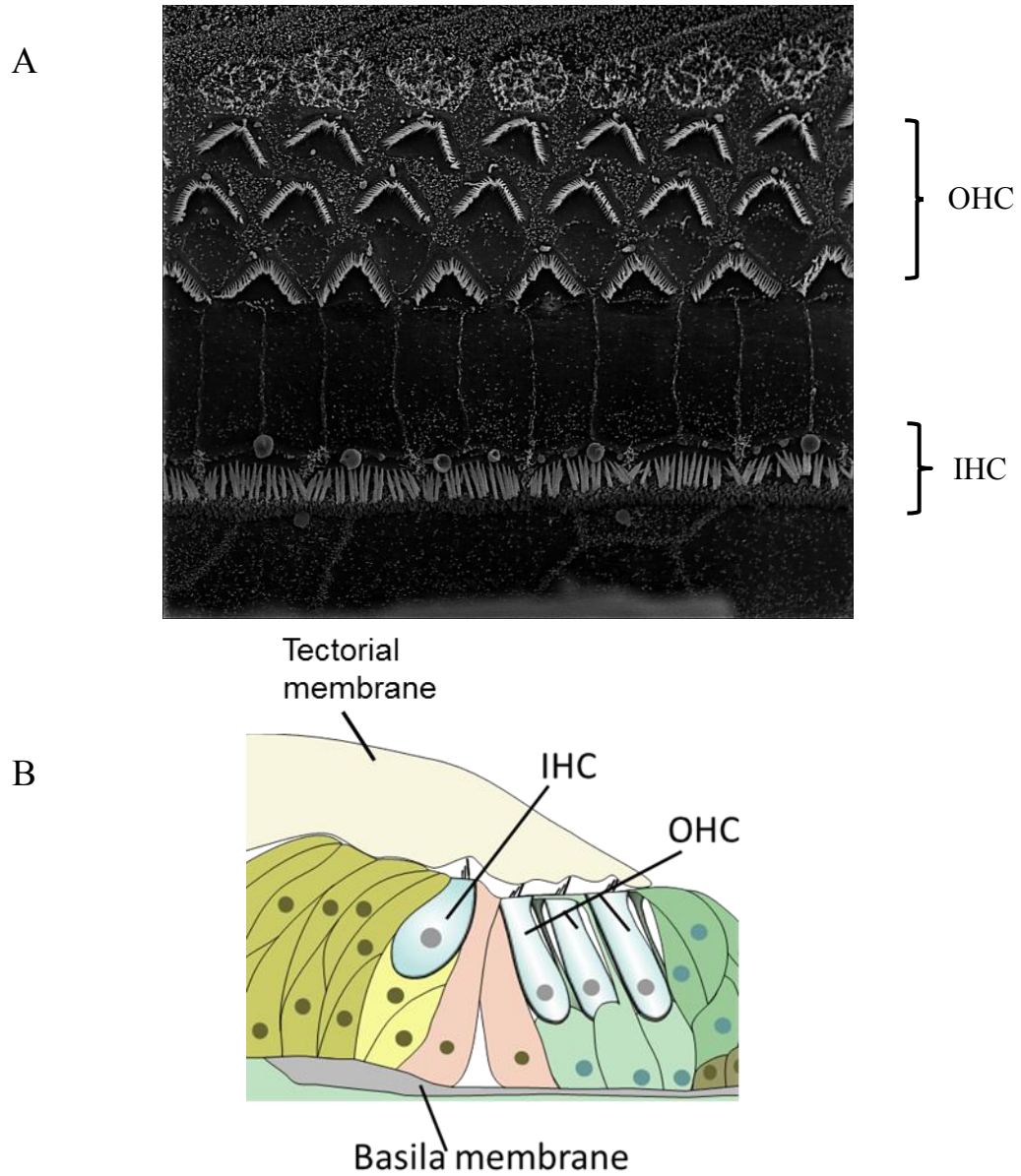


Figure 3.2-3: The Organ of Corti.

- A) SEM image showing the top view of the Organ of Corti.
B) Cartoon showing the hair cells, tectorial membrane and basilar membrane.

Figure 3.2-3 illustrates the top view of a scanning electron microscopy image (A) and a cross section view of the Organ of Corti (B). It comprises a row of inner hair cells (IHCs) and three rows of outer hair cells (OHCs) (Figure 3.2-3: The Organ of Corti., A). Both these types of hair cells are mechanosensory but they differ in structure and function. Stimulation of inner hair cells results in transducing mechanical energy of sound waves into electrical signals that are transmitted to the brain via vestibulocochlear nerve. In Figure 3.2-3: The Organ of Corti., B at the basal region of the hair cells, there are different types of supporting cells and basilar membrane. Right above the apical region of the hair cells, the tectorial membrane is located. Each of those parts of the Organ of Corti will be briefly described below.

Basilar membrane is located basally relative to the supporting cells. It has several properties, like width, thickness, stiffness and damping factor, that vary along the length of the organ of Corti. For example, the basal membrane increases in thickness, but decreases in stiffness from base to apex. This gives the organ of Corti tonotopic characteristics, i.e. certain regions in it can be stimulated by a tone of specific frequency, and so it has been found that high frequencies cause movement of the basal membrane at the base of organ of Corti while lower frequencies cause movement at the apex.

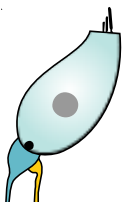
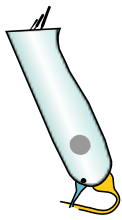
IHCs and OHCs differ in function. IHCs are the sound-detecting cells. In rodents, hearing ensues when IHC, which function as the cellular receptors of sound, mature around Postnatal day 10-14 (P10-P14) (20). They form a single row of cells and are innervated by afferent neurons of the spiral ganglion from their basal region. Both, IHCs and OHCs have on their apical region, two important structures: a microvilli-like projections known as stereocilia which function as mechanical transducers and a cuticular plate made of a dense network of actin where the stereocilia are inserted.

OHCs form three rows of cells and are known for their electromotility function that enhances the cochlea's sensitivity and frequency selectivity and so they are considered as "cochlear amplifiers". A specific protein, Prestin, is found in OHCs but not IHCs and surrounds the cell body laterally and is thought to cause the contraction and

electromotility of OHC in a voltage-dependent manner (21). OHCs reach functional maturity around P8 (20).

Both types of hair cells do not regenerate once damaged, either due to chemicals such as certain antibiotics, trauma from loud noise or just old age. The cell bodies of both types are surrounded by perilymph while their stereocilia is bathed in endolymph. The hair cells are surrounded by many types of supporting cells: Pillar, Deiters', Caludius and Hensen's cells to name a few. Supporting cells have an important role in structural support of the hair cells. Table 3.2-1: Summary of compares the differences between OHCs and IHCs.

Table 3.2-1: Summary of differences between OHCs and IHCs.

	IHC	OHC
Shape		
Enervation	Afferent	Efferent
Cell rows	One	Three
Function	Transduces the intensity and frequency of sound waves into electrical signal.	Amplification of sound wave stimuli.
Transduction	Yes	Yes
Electro-motility	No	Yes
Length	Does not vary along the cochlea.	Varies along the cochlea (cells increase in length and decrease in thickness from base to apex).
Regeneration if damaged	No	No

In wild type hair cells, stereocilia form a specific staircase architecture. This architecture may be essential for detection of mechanical deflections to the nanometer scale (13) and transduction of the mechanical energy of sound waves into electrical signals via the mechano-electrical transduction (MET) channels that are located at the tips of stereocilia. The structure of stereocilia and mechanism of transduction and their role in amplification and hearing will be described with more details in a later section.

Located right above the stereocilia is the tectorial membrane. It is a gel-like membrane composed of a mix of collagen, glycoproteins and proteoglycans, but most of its weight is water. It functions as a means of stimulation for the hair cells by deflecting their stereocilia during sound-induced vibration.

3.3 Myosin proteins

There are at least 18 known classes of Myosins in their super-family (22). Each class has specific function in the cell ranging from cytokinesis to trafficking and signal transduction. In general, they have a general structure with highly preserved functional domains:

- **Motor (head):** mostly conserved in all classes, binds to actin and ATP. (23)
- **Neck:** contains IQ motif that binds calmodulin. (23)
- **Tail:** at the C-terminal, anchors the motor domain, varies between classes. Contains motifs that bind to other proteins, like SH3 and MyTH4-FERM (23).

Myosin can be classified into two large groups; conventional and unconventional. Conventional myosin, best example is Myosin 2, is found in muscle cells (skeletal, cardiac and smooth) and are involved in contraction. Unconventional myosin (Myosin 6, 7, 15) have variable structures and functions in the cell, for example they are involved in vesicles transport in the cell (24) and, in the inner ear hair cells, Myosin 15a interacts with the actin core of stereocilia through its motor domain and also through actin-binding proteins like Eps8. Myosin 15a is thought to have an important function in developing

graded length of stereocilia rows in the hair cell bundle and in maintaining stereocilia length by interacting with scaffolding proteins like Whirlin.

3.3.1 Myosin 15a

Myosin 15a is an unconventional motor protein found at the tips of stereocilia in both inner and outer hair cells of the inner ear and also in some neuroendocrine and endocrine tumor cells. Myosin 15a is encoded by chromosome 17 in human. Its analog in mouse is on chromosome 11 and has 66 exons (4). It is predicted that there are at least 30 Myosin15a proteins are transcribed from alternatively spliced mRNA. In general, there are two sub-classes of *Myosin15a* transcripts; class1 and class 2 which differ in size (10,5kb and 6.9kb, respectively). Class 1 is transcribed starting with exon 2 through exon 66 and skipping exon1, while class2 is transcribed starting with exon 1 through 66 and skipping exon 2(3). Figure 3.3-1: shows the structure of Myosin15a. It has a motor domain, IQ motif, two MyTh4, two FERM and two SH3 motifs and a PBD motif at its C-terminal. It can also have a long N-terminal. Mutation in the motor of Myosin 15a causes the congenital DFNB3 type of deafness in humans and same mutation causes deafness and vestibular defects in *Myo15^{sh2/sh2}* mice (25) which will be discussed in a later section.

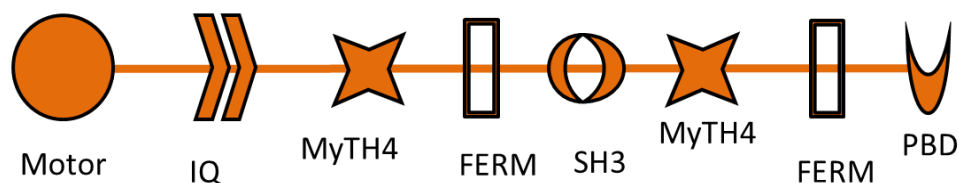


Figure 3.3-1: Structure of Myosin15a. It has a motor domain, IQ motif, two MyTh4, two FERM an SH3 motif and a PBD motif at its C-terminal.

It has been shown that Myosin 15a has an important role in maintaining the staircase structure of stereocilia of both the inner and outer hair cells (25). It has the highly conserved motor domain that binds to actin and other functional domains that bind to cargo protein, whirlin, and transports it to the tips of stereocilia using energy produced from ATP hydrolysis (Figure 3.3-2: Myosin15a is located at the tips of hair cell

stereocilia and interacts with actin, whirlin, and the actin-binding protein Eps8.).

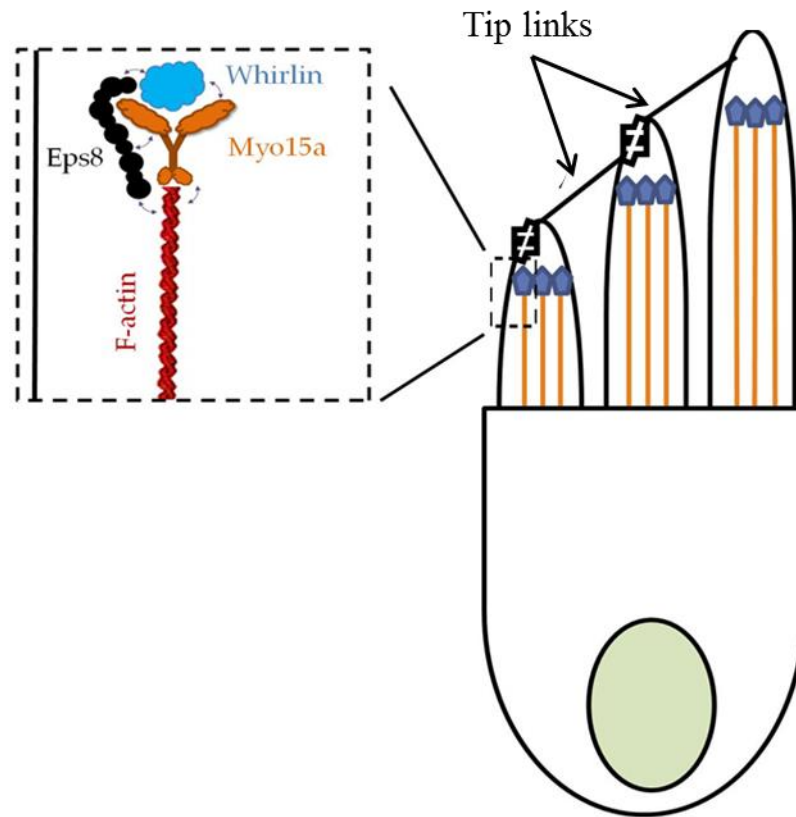


Figure 3.3-2: Myosin15a is located at the tips of hair cell stereocilia and interacts with actin, whirlin, and the actin-binding protein Eps8. Myosin 15a maintains the normal staircase structure of stereocilia bundle.

3.3.2 Myosin 15a interaction with Whirlin and other proteins

Whirlin is a cargo and scaffolding protein known to interact with Myosin15a and other transmembrane proteins and is also found at the tips of stereocilia in wild type mice. It consists of class 2 PDZ ligand, three PDZ domains and a proline-rich domain. *Whrn*^{wi/wi} mice lack whirlin protein, are deaf and have short stereocilia. (26)

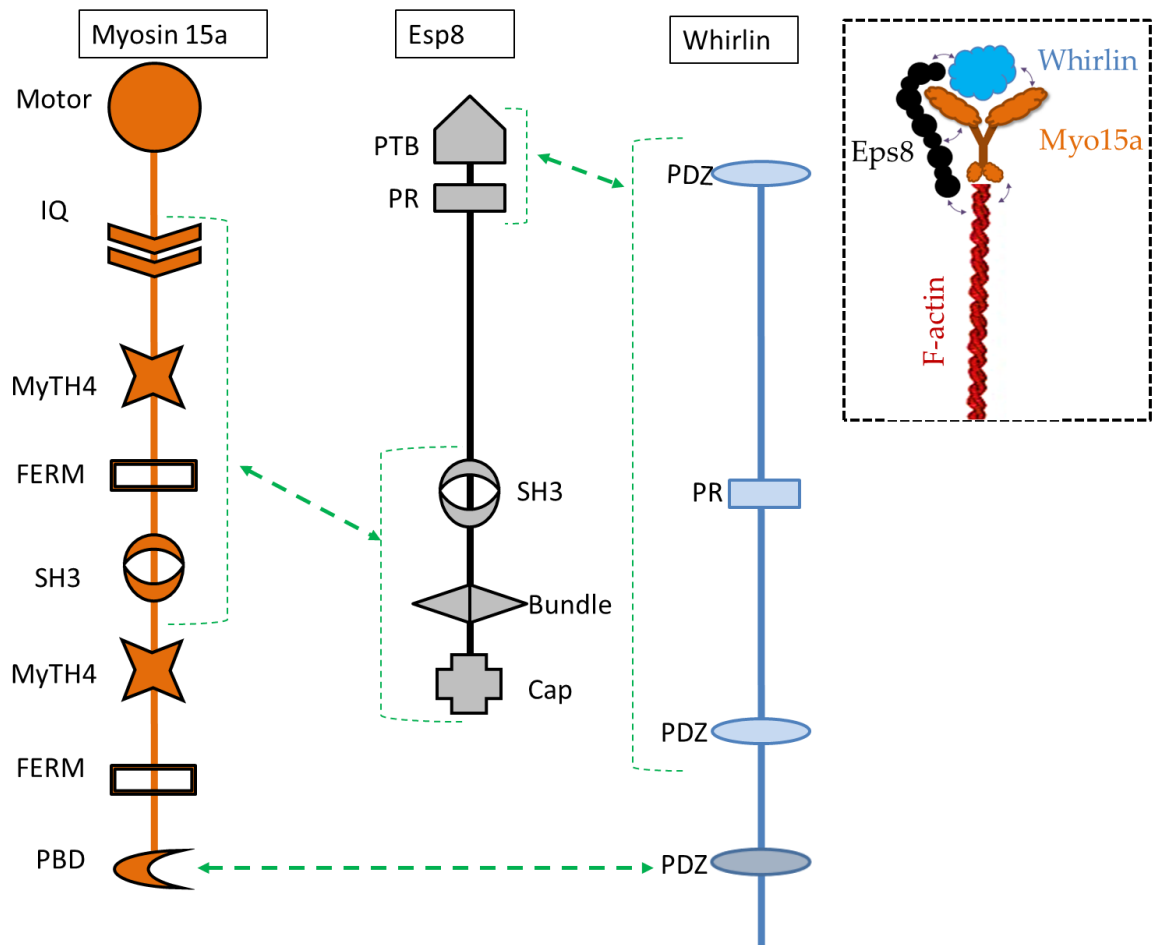


Figure 3.3-3: The interaction between domains of Myosin15a, Whirlin and Eps8.

Whirlin is transported to the tips of stereocilia by Myosin 15a, as shown in Figure 3.3-3: The interaction between domains of Myosin15a, Whirlin and Eps8. Belyantseva et al show that *Whrn*^{wi/wi} mice have Myosin 15a at their tips but not whirlin, while *Myo15*^{sh/sh} lack either proteins at their tips and whirlin is found in the cell body. PDZ class 1 domain of Whirlin is thought to interact with PDZ class 1 ligand of Myosin 15a. It has been shown that Myosin 15a with a deleted PDZ ligand is found at the tips of the stereocilia but whirlin protein remains in the cell body. (26)

Manor et al, (27) showed that Myosin 15a interacts with the actin-binding proteins, Eps8. In order to investigate how they interact, Manor et al., created an Eps8 that lacks SH3, the actin binding and capping domains. They found that the lack of SH3 disrupted Eps8 interaction with many proteins and resulted in short stereocilia. Using

immunofluorescence labeling, Manor et al, showed that in *Myo15^{sh2/sh2}* mice, Eps8 was absent from the tips of stereocilia and was reduced in *Whrn^{wi/wi}* mice. They concluded that Myosin15a interacts with Eps8 through at least one motif, MyTh-4-FERM, with the C-terminal of and is required for its transportation to the tips of stereocilia, while Whirler stabilizes Myosin15a:Eps8 complex.

3.4 Mechanotransduction

MET channels in both OHCs and IHCs transduce the mechanical energy of the sound-induced waves into an electrical signal. The MET channel is gated mechanically by tensioned tip links. When the stereocilia are deflected towards the tallest row, the channels open and the cell depolarizes, while deflecting them in the opposite direction closes the channel and the cell hyperpolarizes. The loss of tip link disrupts mechanotransduction, while their restoration reinstates the activity of the MET channel (28).

The exact molecular structure of the MET channel in the inner ear is unknown, yet many of its characteristics have been measured. It has been shown that it has rapid activation kinetics (in microseconds). It also shows adaptation upon activation. Its conductance varies tonotopically along the cochlea from 100 to 300pS (8; 29; 30). The MET channel is a voltage-independent (10), non-specific cation channel with higher permeability for Ca^{2+} (12). Using pharmacological blockers of MET channel can help in comparing its characteristics with those of known channels. Open MET channel can be blocked using drugs like aminoglycosides, amiloride and their derivatives. MET channels co-localize at the tips of stereocilia with Myosin15a (Figure 3.4-1:), but Myosin 15a is not required for mechanotransduction. Stepanyan et al., (5) showed that IHC and OHC of young *Myo15^{sh2/sh2}* mice have intact mechanotransduction current even though they are missing Myosin15a.



Figure 3.4-1: MET channel is gated directly or indirectly by a tensioned tip link and is co-localized at the tips of stereocilia with Myosin15a.

Image used with permission of Zubair M et al., *Physiological genomics* (2013) (31).

3.5 Mechanoelectrotransduction channel blockers

3.5.1 Amiloride

Amiloride was first used in treating hypertension and managing congestive heart failure. It is a Potassium-sparing diuretic that spare the potassium from being excreted in the urine. Its molecular structure is consisted of a guanidinium group containing pyrazine derivative. Its mechanism of action is based on blocking the voltage-independent epithelial sodium channel (ENaC) with high affinity ($K_d < 1\mu\text{M}$) (32).

Anti-bodies against Amiloride-sensitive ENaC showed immune-staining at the tips of stereocilia where the MET channel is thought to be found. In addition, Amiloride was used to reversely-block the transducer channels in chick hair cells. These two observations serve to suggest that amiloride might also block MET channel (33). The work of Kros et al, (33) looked into the structure-activity relationship in the MET channel and its gating mechanism. They showed that amiloride and its derivatives could block the MET channels in a neonatal mouse cochlea but this blockage does not involve specific binding. The drug enters from the extracellular solution into the pore of the channel and blocks it in a voltage-dependent (bottle-cork) manner.

3.5.2 Dihydrostreptomycin

The antibiotic Dihydrostreptomycin (DHS) belongs to the Aminoglycosides group that includes streptomycin, gentamycin, kanamycin and others. Historically, the group was first used to cure tuberculosis in the late 1940 (34). It was later discovered that patients who took these antibiotics presented chronic nephrotoxic and ototoxic symptoms. The exact part of the molecular structure that causes ototoxicity is unknown (34). The drug causes death of OHC on the basal part of the Organ of Corti then progresses to the apical part. It is also noticed that OHCs are more susceptible to the drug than IHCs. Kroese et al (1989) (35) used DHS to reversibly block the transduction channel in the bullfrog

sacculus. They showed that the half-blocking concentration of aminoglycosides is in the range of 2-95uM.

The mechanism of blocking for both compounds is “bottle cork”; they block the MET channel from the extracellular region (Figure 3.5-1: MET channel blocked by blockers in a “bottle cork” mechanism.-1).

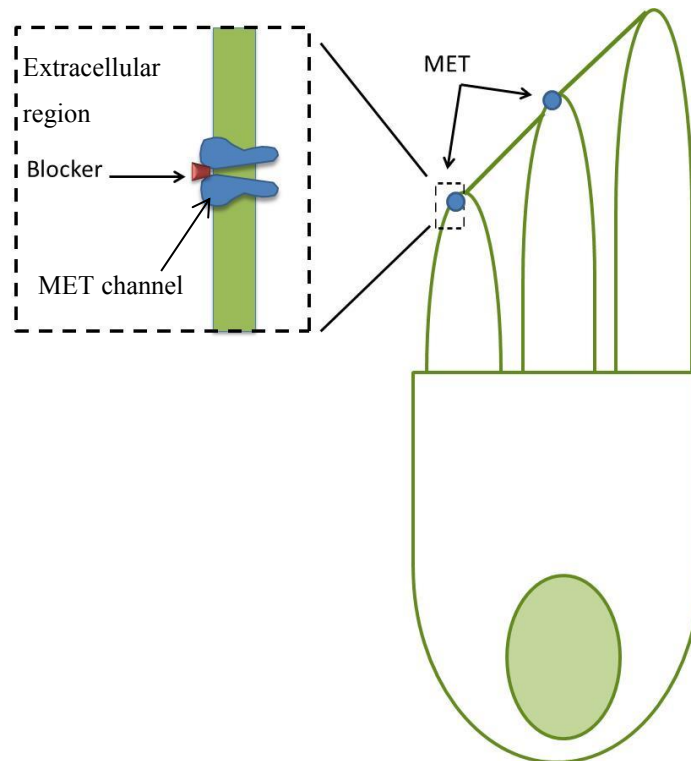


Figure 3.5-1: MET channel blocked by blockers in a “bottle cork” mechanism.

3.6 Genetics of deafness

It is estimated that about 1% of human genes are necessary for hearing (36). In many cases, children with normal hearing that are born to deaf parents suggest that there are different genes whose mutation could cause deafness. This indicates how diverse the proteins involved in this sense. Deafness can be either syndromic (is one of the symptoms of a disease) or non syndromic (not associated with any disease).

Most documented mutations that cause nonsyndromic hearing loss is caused by mutations in a single gene (36). Those can be autosomal dominant, autosomal recessive, or sex-linked. For the purpose of this thesis, an autosomal recessive mutation will be the main point of discussion.

3.6.1 Non-syndromic congenital sensorineural deafness

The conventional nomenclature for autosomal dominant mutation that results in nosyndromic deafness is DFNA, while DFNB refers to the autosomal recessive mutation and accounts for 85% of prelingual deafness (37). The number following a type of non-syndromic deafness indicates which locus is affected. For example, DFNB3 is the main focus of this work, refers to the locus *DFNB3* on chromosome 17 that encodes for unconventional Myosin15a (4).

3.6.2 DFNB3 deafness

A gene first identified in a village in Bengkala, Bali (2) where 2 % of the villagers have congenital, nonsyndromic neurosensory profound deafness. Later on, it was also found in other communities like India (36) (4), Pakistan (36) where consanguineous marriages are common. Thomas Friedman et al, (2) hypothesized that deafness is caused by an autosomal recessive mutation in this particular gene and it is a result of a founder effect. Because of the high incidence level in Bengkala, seven affected generations, the villagers have adapted a unique and complex sign language known as Kata Kolok (translation: deaf talk) (38) that is known by both the hearing and the deaf and is different from the Indonesian sign language.

DNA analysis of deaf individuals shows that they have an autosomal recessive mutation at the *DFNB3* locus. The technique used to locate this locus on human chromosome was an integration of association mapping strategy, analysis of historical recombinants and a derivation of Genome-wide homozygosity mapping known as allele-frequency-dependent homozygosity mapping (AHM) (2). The result was that *DFNB3* was mapped on chromosome 17 and was later refined to 17p11.2 and suggested that DFNB3 has multiple alleles that could have two independent mutations (4). Work done by Wang et al, associated DFNB3 deafness with mutations in *Myo15a* (39) (4).

3.7 Shaker2 mouse model

Shaker-2 (*Sh2*) mutation was suggested to be homologue to *DFNB3* based on conserved synteny (2) (4). *Sh2* is comprised of 66 exons spanning 59 kilobases (kb) of DNA on chromosome 11qB2 and has been shown to encode Myosin 15a (40). The human ortholog has the same exon composition distributed across 71 kb on chromosome 17p11.2 (41). Using positional cloning, investigators showed that a missense mutation that changes the amino acid Cysteine (C) to Tyrosine (Y) in the conserved region of the motor domain was present in *Myo15*^{sh2/sh2} mice but not in wild-type mice (37).

These mice have the phenotype of profound deafness and lack Preyer (startle) reflex. Their OHC stereocilia degenerates with age (Figure 3.7-1: Degeneration of stereocilia with age in *Myo15*^{sh2/sh2}) and, unlike humans, have vestibular defects, tossing of the head and circular motion (6). However, the mutation has been corrected using a Helios® gene gun mediated transfection with better results than using other methods of transfection. In this particular method, gold particles coated with cDNA of wild type Myosin 15a and GFP were accelerated using pressurized helium and by so were transfected into the mutated explants. The result was that the stereocilia of OHCs elongated to normal length, staircase phenotype was restored and immunostaining imaging detected Myosin 15a at the tips (42).

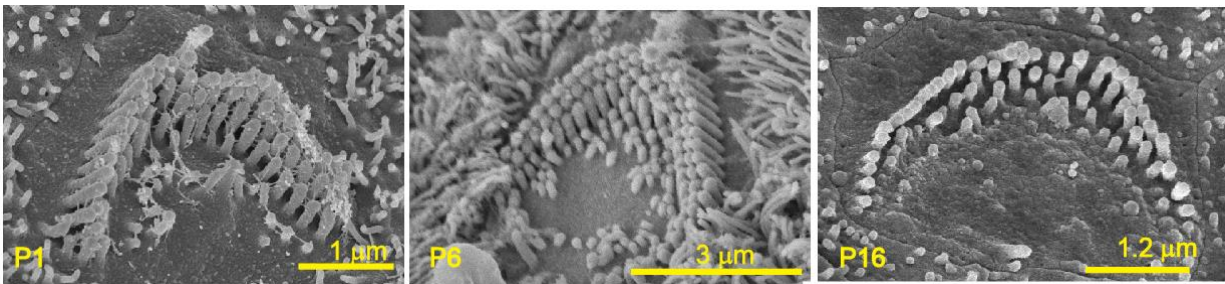


Figure 3.7-1: Degeneration of stereocilia with age in *Myo15*^{sh2/sh2}

3.8 Thesis Objective

The original goal of this study was to investigate the existence of a potential “standing current” in *Myo15^{sh2/sh2}* OHCs with different methods. First, investigation of fast uptake of FM1-43FX dye into the *Myo15^{sh2/sh2}* OHCs was planned to reveal the MET channels that are partially open at rest. Next, whole cell patch-clamp recording were planned to determine the resting ionic conductance in *Myo15^{sh2/sh2}* and *Myo15^{+ /sh2}* OHCs that are sensitive to either Dihydropyridine (DHP) or Amiloride (Amil), the known blockers of MET channels. Finally, we also planned to count stereocilia links in degenerating *Myo15^{sh2/sh2}* OHCs using scanning electron microscopy (SEM) images. Indeed, the experiments revealed “standing current” in *Myo15^{sh2/sh2}* OHCs but, in addition, an unexpected increase in voltage-gated outward conductance that has been also investigated.

Chapter 4 Material and Methods

4.1 Cochlea dissection

Myo15^{sh2/sh2} and *Myo15^{+/sh2}* mouse pups were euthanized at postnatal days 3-5 (P3-P5) by putting them on ice in a cold chamber to induce hypothermia for 4 minutes then decapitated. The skull bone is removed and placed in a dish with (L-15) solution containing the following inorganic salts (in mM): NaCl (137), KCl (5.4), CaCl₂ (1.26), MgCl₂ (1.0), Na₂HPO₄ (1.0), KH₂PO₄ (0.44), MgSO₄ (0.81), pH=7.36, osmolarity = 313 mOsm. The skull is cut across the sagittal suture, from occipital region to give the left and right halves of the skull to access the interior side of temporal bone. The brain tissue was removed to reveal the middle cranial fossa, the excess bones (parietal and occipital) are removed, the porus acusticus internus is opened to reveal the bony labyrinth. Because of the young ages of mice, the bones are not yet ossified and it is easy to open the cochlea without damaging the Organ of Corti. With a swirling upwards motion, the Organ of Corti is removed from the lamina spiralis ossea and is cultured in glass-bottomed dishes with 2ml DMEM media with 7% Fetal Bovine Serum and (10mg/L) Ampicillin. For patch-clamp purpose, the cultured tissue (from now on designated as explants) was held down onto the dish by using two glass pipettes as a “clip” so that culture remains attached to the bottom of the dish. The middle region of the Organ of Corti is placed between the two pipettes so that it can be accessed easily by the patch pipette (Figure 4.1-1). The explants were incubated at 37C and 5% CO₂ for 3-5 days making the equivalent age of explants between P6-P10. After this period, the explant would be attached to the bottom of the dish. All animal procedures were approved by the University of Kentucky Animal Care and Use Committee.

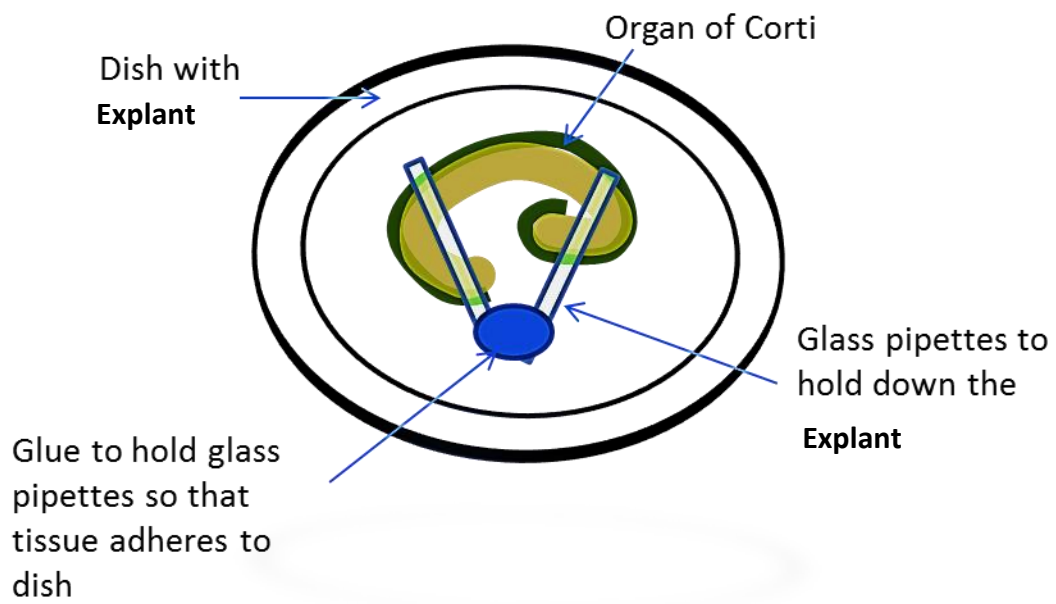


Figure 4.1-1: Culturing the Organ of Corti explant.

4.2 Mouse genotyping

Based on the known phenotype of *Myo15*^{+/sh2} mentioned previously, we can determine the genotype of the specimen even before sending tail snips for PCR (polymerase chain reaction) analysis. Starting from P5, it is possible to distinguish between the control and the mutant IHCs by imaging them with high-resolution optical microscope (Nikon E600FN) equipped with DIC (differential interference contrast). Stereocilia bundles of *Myo15a*^{+/sh2} IHCs have clear staircase architecture that can be identified by changing the focal plane. In contrast, stereocilia of *Myo15*^{sh2/sh2} IHCs are much shorter and have the same length. In addition, *Myo15*^{sh2/sh2} IHC bundle have extra numerous stereocilia that are failed to retract in postnatal development (Figure 4.2-1).

Alternatively, we dissected vestibular organs of the same animals, opened the ampullae and examined stereocilia bundles of the vestibular hair cells with high-resolution upright microscope (Nikon E600FN). Because vestibular hair cells in the ampullus have very long stereocilia (tens of micrometers), the unusually short stereocilia in *Myo15*^{sh2/sh2} mice are easily noticeable.

Examination of stereocilia length allowed us to determine the genotype in a live specimen, before patch-clamp experiments. The genotype was then confirmed by PCR analysis of tail snips.

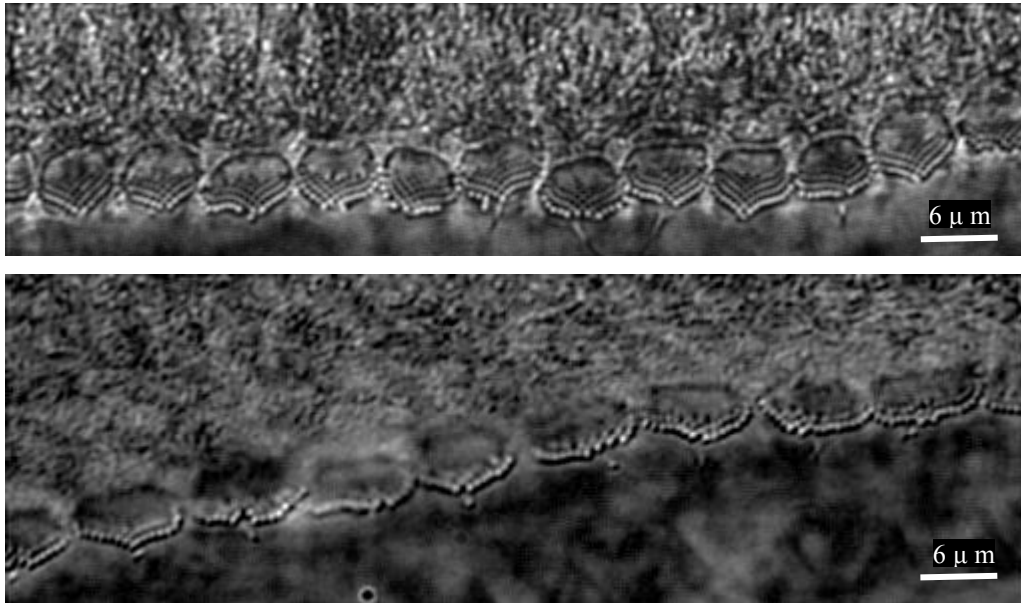


Figure 4.2-1: The difference between *Myo15*^{sh2/sh2} (top) and *Myo15*^{+/sh2} (bottom) IHCs can be observed by optical microscopy at P4+4 days in vitro (div). Hair bundles of *Myo15*^{sh2/sh2} IHCs have equally short stereocilia and extra rows of stereocilia. Images were obtained with high-resolution optical microscope (Nikon E600FN) equipped with DIC.

4.3 Counting stereocilia links

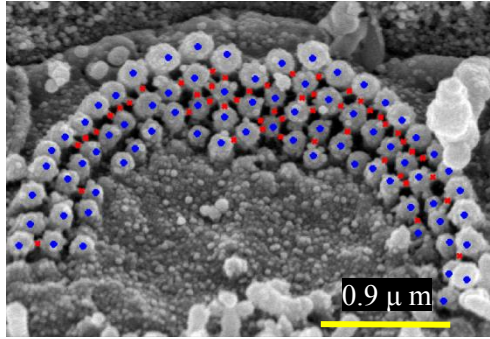


Figure 4.3-1: Counting links (red dots) and stereocilia (blue dots) in a *Myo15^{sh2/sh2}* OHC.

To quantify degeneration of stereocilia links in *Myo15^{sh2/sh2}* OHCs, the number of links per stereocilium was determined in *Myo15^{sh2/sh2}* OHCs at different age. Figure 4.3-1 shows scanning electron microscopy (SEM) image of an OHC at P9. Using a MATLAB script, SEM images were loaded into MATLAB and then links (red dots) and stereocilia (blue dots) were manually selected and counted.

4.4 Fluorescent imaging with FM1-43FX

To test whether *Myo15^{sh2/sh2}* OHCs in older mice (P26) have functional MET channels that partially open at rest despite loss of their tip links, the Organ of Corti was briefly exposed to FM1-43FX (Invitrogen), a fixable analog of non-toxic and water-soluble lipophilic styryl dye FM1-43. Then, the specimen was fixed before dissecting; otherwise the hair cells would be damaged. The excitation and emission wavelengths of FM1-43FX are the same as the ones for FM1-43 (excited at 510nm and emits a green fluorescence at 626nm).

A small hole at the apical region of the cochlea was made. Immersing the dissected cochlea in cold L-15 solution (3-4 °C) for 45seconds ensures that endocytosis is slowed down or even stopped (Figure 4.4-1: Labeling hair cells with FM1-43FX. (A) Arrangement of the perfusion pipette relative to the hole at the apex of the cochlea. (B) Perfusion flow replaces intracochlear fluids.). A working solution of 3uM FM1-43FX is prepared and is used to perfuse the cochlea for 40 seconds. Perfusion can be seen by movement of the bathing solution at the base of the cochlea (Figure 4.4-1, B). Then, the cochlea is perfused with cold L-15 solution for washout and fixed with 4% Paraformaldehyde solution for one hour. The organ of Corti was carefully dissected, post-stained with Rhodamin Phalloidin to label stereocilia actin, mounted on slides, and viewed with CARV confocal attachment and Hamamatsu ORCA-IIER digital camera.

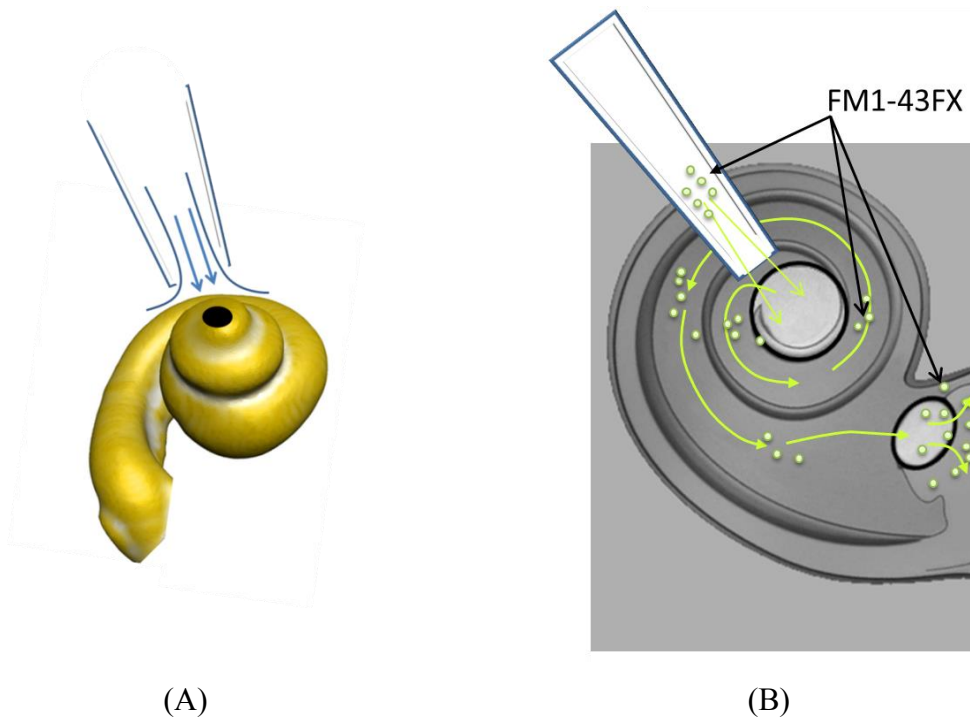
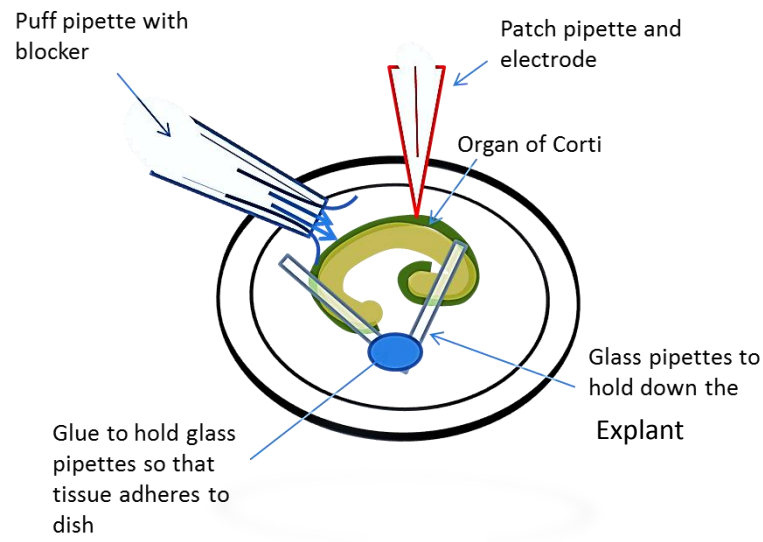


Figure 4.4-1: Labeling hair cells with FM1-43FX. (A) Arrangement of the perfusion pipette relative to the hole at the apex of the cochlea. (B) Perfusion flow replaces intracochlear fluids.

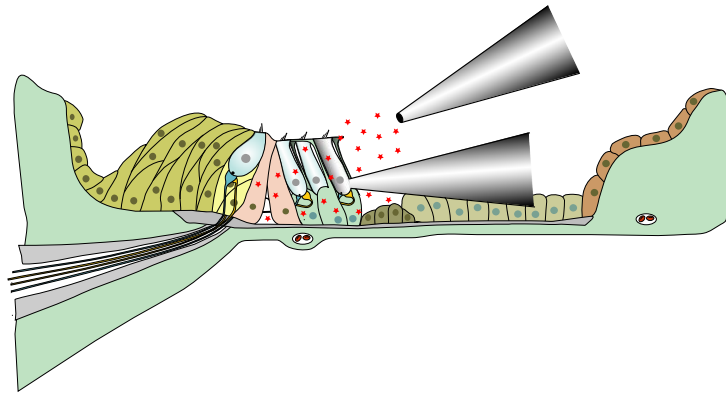
Cochlea image in (A) credits: Wikimedia Commons (43)

4.5 Whole-cell patch clamp

All experiments were performed in Leibovitz (L-15) extracellular medium. The Organ of Corti was observed under (Nikon E600FN) using 60X objective lens. Healthy OHCs were identified by existence of stereocilia at apex of the cell, lack of Brownian motion of mitochondria, normal size (not inflated). (Figure 4.5-1, A) shows the setup for whole cell patch-clamp recordings. The explant was attached to a glass-bottomed dish so that the middle turn of the Organ of Corti can be in direct contact with the patch pipette and is held down onto the dish by two glass pipettes. In order to access and patch the basolateral region of the outermost row of OHCs (Figure 4.5-1, B) the supporting cells (Hensen and Deiters cells) were removed by gentle suction through a glass pipette. The outgrowth of tectorial membrane material was also removed in the same way. Patch pipettes were filled with intracellular solution that contains (KCl (12.6 mM), KGlu (131.4 mM), MgCl_2 (2 mM), EGTA (0.5 mM), K_2HPO_4 (8 mM), KH_2PO_4 (2 mM), $\text{Mg}_2\text{-ATP}$ (2 mM), $\text{Na}_4\text{-GTP}$ (0.2 mM). The osmolarity of this solution was adjusted to 330 mOsm and pH to 7.36 similar to intracellular solution. Patch pipette resistance was typically 4.4-7.4 M Ω when measured in the bath. Patch-clamp recordings were performed with a computer-controlled amplifier (MultiClamp 700B, Molecular Devices). For consistency, only the OHCs in the middle of the cochlea were selected for the experiments.



A



B

Figure 4.5-1: Illustration showing set up and procedure for whole cell patch-clamp recordings. A) Glass-bottom Petri dish with the organ of Corti explant, patch and puff pipettes. B) In order to access and patch the basolateral region of the outermost row of OHCs, the supporting cells (Hensen and Deiters cells) were removed. The MET blocker is applied through a puff pipette that is at 90° with the hair bundles and is 10-15 μ m away to make sure that the bundles are not deflected (Image courtesy: A. Catalina Velez-Ortega).

Blocking of mechanotransduction channels

The drugs blocking MET channels (100uM Amiloride or DHS) are applied using pneumatic injector (DAGAN PMI-200) through a puff pipette that is at 90° with the hair bundles and is 10-15 μm away to make sure that the bundles are not deflected.

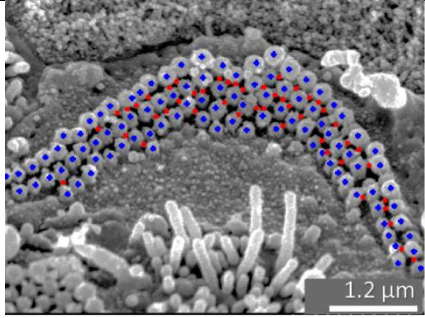
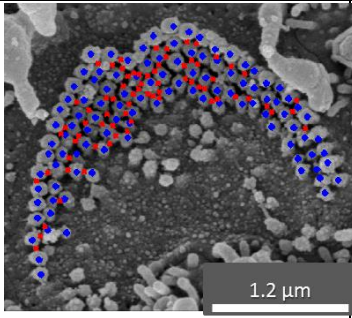
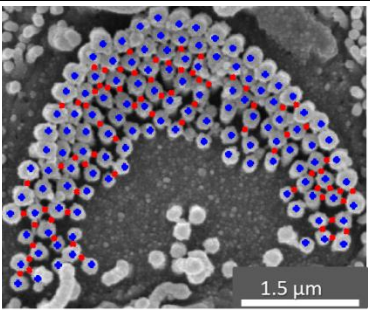
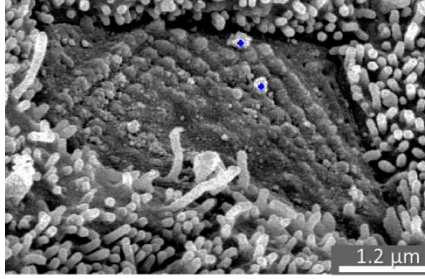
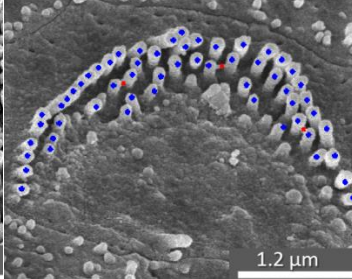
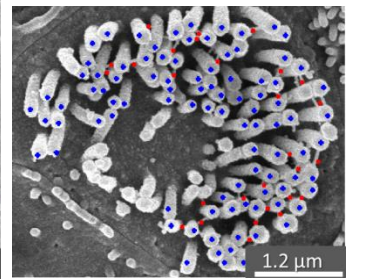
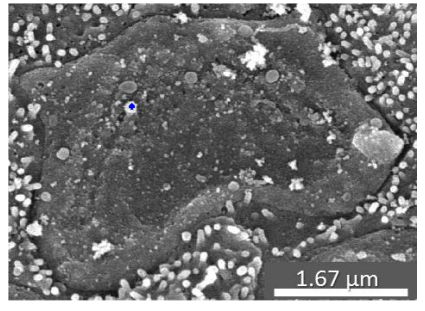
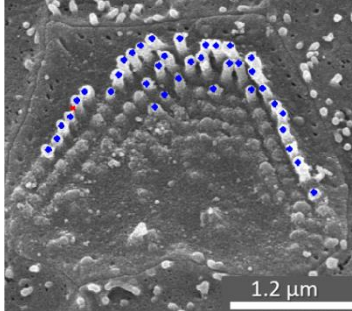
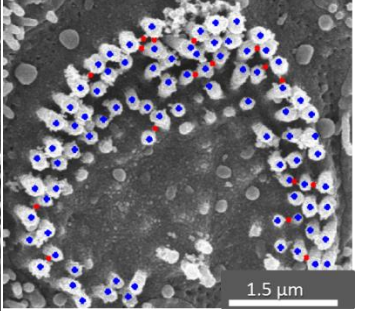
Experimental protocol

While holding the cell's membrane potential at -60mV, the whole cell current is recorded. A voltage-step protocol ranging from -100 to 68 mV is applied and the current response is recorded for the control, blocker application and 15 min after blocker application stopped (washed out).

Chapter 5 Results and Discussion

5.1 Stereocilia links rapidly deteriorate in *Myo15^{sh2/sh2}* mice

Tip links are the tethers that interconnect the tips of the shorter row of stereocilia to the adjacent taller stereocilia. They consist of cadherin-23 and protocadherin-15 adhesion proteins. The tip links are thought to gate the MET channel either directly (attached to the channels) or indirectly (by pulling the cell membrane). Hair cells of young postnatal *Myo15^{sh2/sh2}* mice have tip links that contribute to their mechano-sensitivity. Stereocilia bundles in *Myo15^{sh2/sh2}* hair cells develop normally till about P3. Then, the further growth of stereocilia seems to be “arrested” and OHCs begin to degenerate. Degeneration of stereocilia in *Myo15^{sh2/sh2}* OHCs has a different rate depending on the tonotopic location along the cochlea. Hair cells at the base of the cochlea degenerate at a faster rate than those at the apex of the cochlea. (Figure 5.1-1). Quantification of the number of links per stereocilium in *Myo15^{sh2/sh2}* OHCs shows the prominent decrease of all the links after P3, including the tip links. The number of links per stereocilium in *Myo15^{sh2/sh2}* OHCs becomes rapidly less than the number of tip links in wild type OHCs, which is around 84% (Figure 5.1-2).

	Base	Mid	Apex
P9			
P16			
p-27			
<p>Figure 5.1-1: Degeneration of stereocilia in <i>Myo15^{sh2/sh2}</i> with age has a different rate depending on the tonotopic location along the cochlea. Hair cells at the base of the cochlea degenerate at a faster rate than those at the apex of the cochlea.</p>			

Number of links per stereocilia (%)

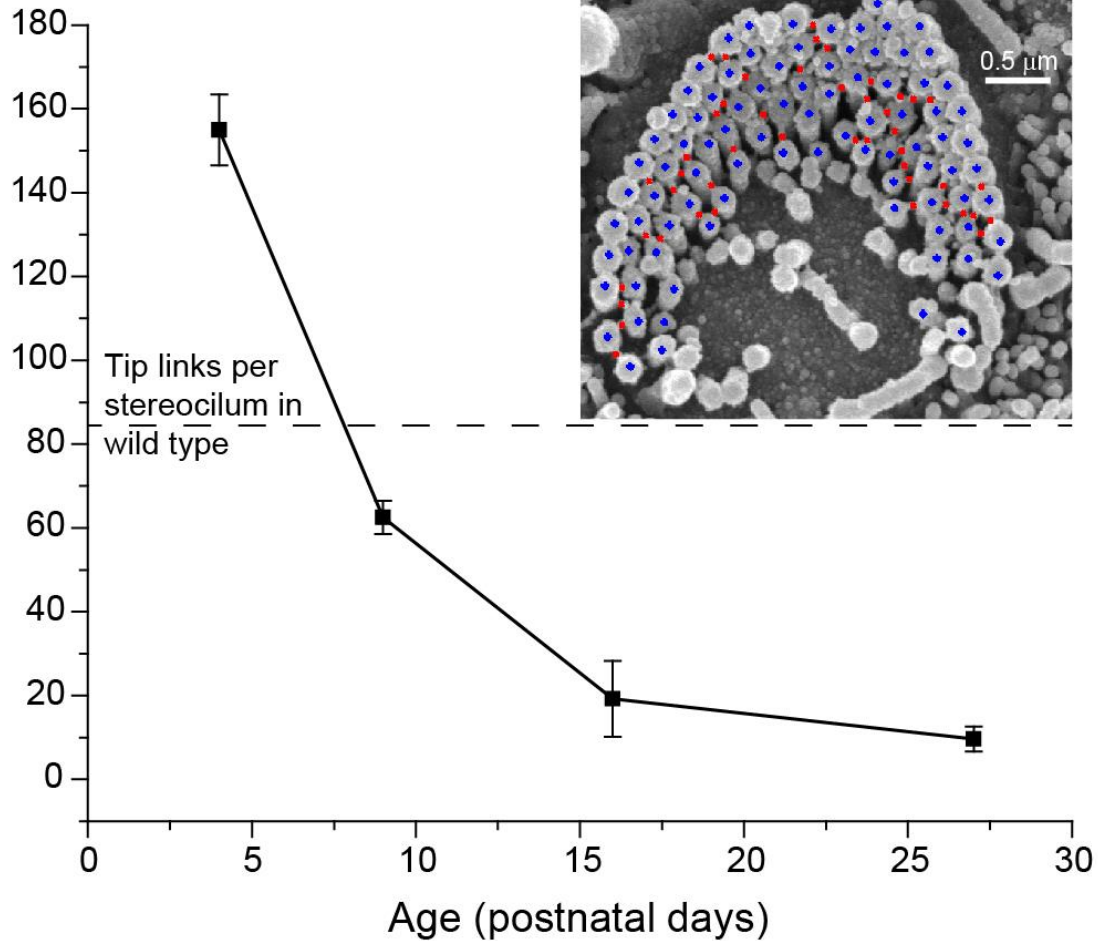


Figure 5.1-2: Progressive loss of stereocilia links in postnatal *Myo15^{sh2/sh2}* outer hair cells with age. Number of links per stereocilium was calculated by dividing the number of all visible links (red dots in the representative SEM image in the inset) to the number of all visible stereocilia (blue dots). The dashed line indicates typical number of tip links per stereocilium in the wild type outer hair cells (44).

5.2 FM1-43FX uptake in *Myo15^{sh2/sh2}* OHCs indicate the presence of constitutively open non-selective cation channels

FM1-43 is mainly used to label plasma membrane, study endocytosis, visualize vesicle trafficking and release of neurotransmitters. When used in the inner ear, the dye labels the plasma membrane of the hair and supporting cells but it is also found in the soma of the hair cells. There are two routes for the dye to get into the hair cell, either by endocytosis or through the MET channels (Figure 5.2-1, A). Gale et al., (45) showed that brief exposure to FM1-43 does not label the hair cells at low temperature (4°C) after tip link disruption but produces strong staining in the hair cells with intact MET apparatus. Thus, brief exposure to FM1-43 at low temperature does not evoke significant endocytosis and can be used to test the presence of functional MET channels that are partially open at rest.

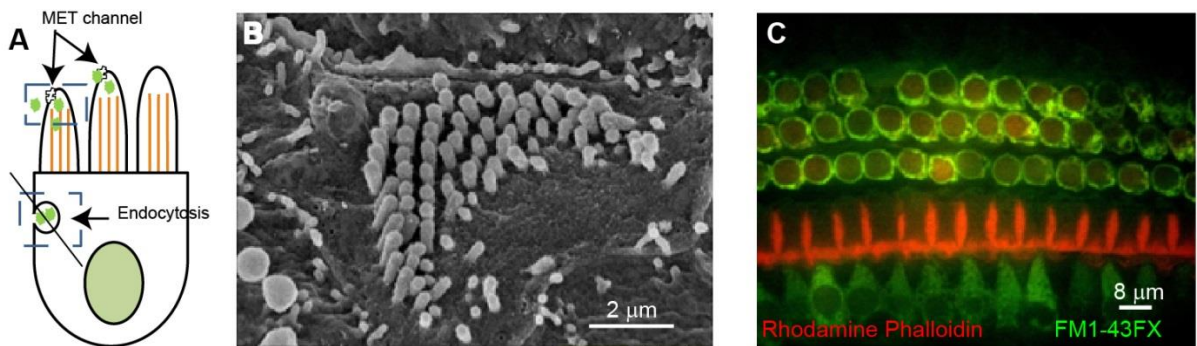


Figure 5.2-1: FM1-43FX uptake in *Myo15^{sh2/sh2}* OHCs indicates the presence of constitutively open non-selective cation channels. (A) SEM image of P25 OHC stereocilia of *Myo15^{sh2/sh2}* mouse. Note the absence of any links between the stereocilia. (B) Confocal image of the organ of Corti of *Myo15^{sh2/sh2}* mouse of the same age showing the uptake of the dye (green) into the OHCs. Rhodamin-phalloidin stains the actin filaments (red).

To test whether the disappearance of stereocilia links in the OHCs of the older *Myo15^{sh2/sh2}* mice (P25) resulted in the permanent closure of the MET channels, we have perfused the organ of Corti explant with cold (4°C) FM1-43FX fluorescent dye. At that age, all tip links between stereocilia have been lost, as it is seen in the SEM image (Figure 5.2-1: FM1-43FX uptake in *Myo15^{sh2/sh2}* OHCs indicates the presence of constitutively open non-selective cation channels. (A) SEM image of P25 OHC stereocilia of *Myo15^{sh2/sh2}* mouse. Note the absence of any links between the stereocilia. (B) Confocal image of the organ of Corti of *Myo15^{sh2/sh2}* mouse of the same age showing the uptake of the dye (green) into the OHCs. Rhodamin-phalloidin stains the actin filaments (red)., B). Because endocytosis is very unlikely to occur at 4°C and because the incubation time was rather short (45 seconds), the FM1-43FX is likely to enter OHCs and IHCs through constitutively or partially open non-selective cation channels, e.g. MET channels (Figure 5.2-1, C). We concluded that the MET channels are still open at rest, at least partially, in the *Myo15^{sh2/sh2}* OHCs even after degeneration of their stereocilia links.

5.3 *Myo15^{sh2/sh2}* mutation results in an increased outward current in OHCs and a more negative intracellular potential

Figure 5.3-1: shows the whole cell current responses to the consecutive voltage steps ranging from -100 to +68 mV in *Myo15^{+/sh2}* (A) and *Myo15^{sh2/sh2}* (B) OHCs. The current-voltage (I-V) relation measured at the “steady state” (100–122 ms of voltage step) and the intracellular voltage are seen in (C). The I-V curve indicates that, on the negative part of the curve, the two current are not significantly different while on the positive part of the curve, the mutant OHCs (red) possess larger outward control current than the OHCs in littermate heterozygous mice (blue). The increase in the outward current in mutant OHCs correlates well with the statistically significant changes of the reversal (intracellular) potential (V_{rev}). V_{rev} in mutant OHCs (red) was more negative than the control (blue). We concluded that myosin 15a-deficiency results not only in abnormally short stereocilia but also in the increase of voltage-gated outward conductance. This

conductance is consistent with the outward K^+ current, because it increases the negative intracellular potential toward the K^+ equilibrium.

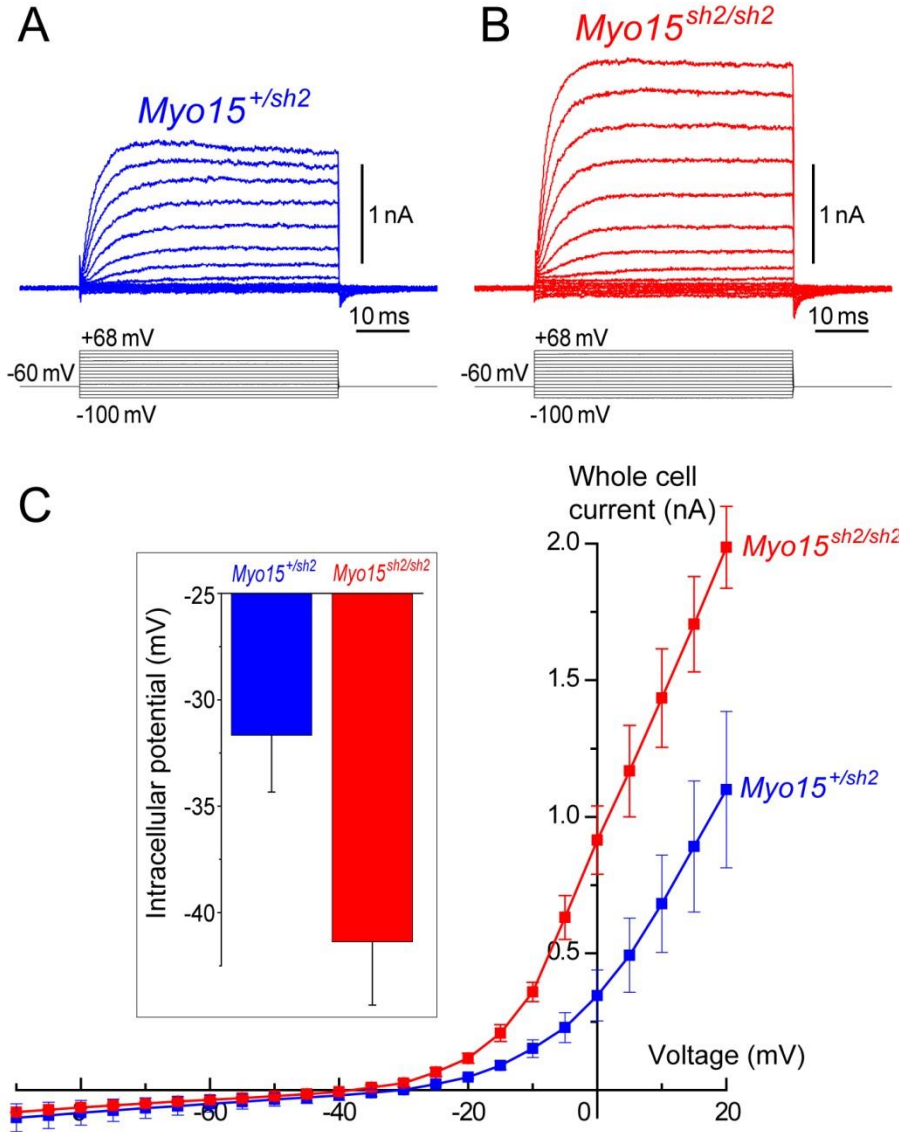


Figure 5.3-1: Ionic currents in *Myo15*^{+/sh2} (A) and *Myo15*^{sh2/sh2} (B) OHCs (upper traces) evoked by the graded voltage steps (lower traces). (C) The current-voltage relationship (an I-V curve) of the steady-state current in *Myo15*^{+/sh2} (blue) and *Myo15*^{sh2/sh2} (red) OHCs. Data are shown as Mean±SE. The difference at positive potentials is highly significant ($p < 0.0566$, t -test). Number of cells: $n = 14$ (*Myo15*^{+/sh2}), $n = 18$ (*Myo15*^{sh2/sh2}). Age of the cells: P3-5 + 1-5 div. The inset shows the reversal (intracellular) potential in these groups of cells. The difference in reversal potential is also significant ($p < 0.0206$, t -test).

5.4 Blocking of MET current revealed the “standing current” in *Myo15^{sh2/sh2}* OHCs and potential Ca^{2+} -dependent modulation of the voltage-gated outward current

To test the contribution of the MET current to the total current in the cell, we used known drugs that block MET channels: DHS and Amiloride. Figure 5.4-1 shows the effect of applying the blocker DHS and Amiloride in *Myo15^{+/sh2}* (blue) and *Myo15^{sh2/sh2}* (red) OHCs. The effect of the drug can be recognized by observing a reduction (upward change) in the holding current and the termination of blocker application is recognized by returning of the current to base level (downward change) in panels A and C. Corresponding current responses to the previously used voltage-step protocol are shown in (B) and (D), respectively. Values of cell parameters (membrane capacitance, Access resistance, membrane resistance and membrane's time constant) before applying the blocker, during its application and washout are shown in Appendix A.

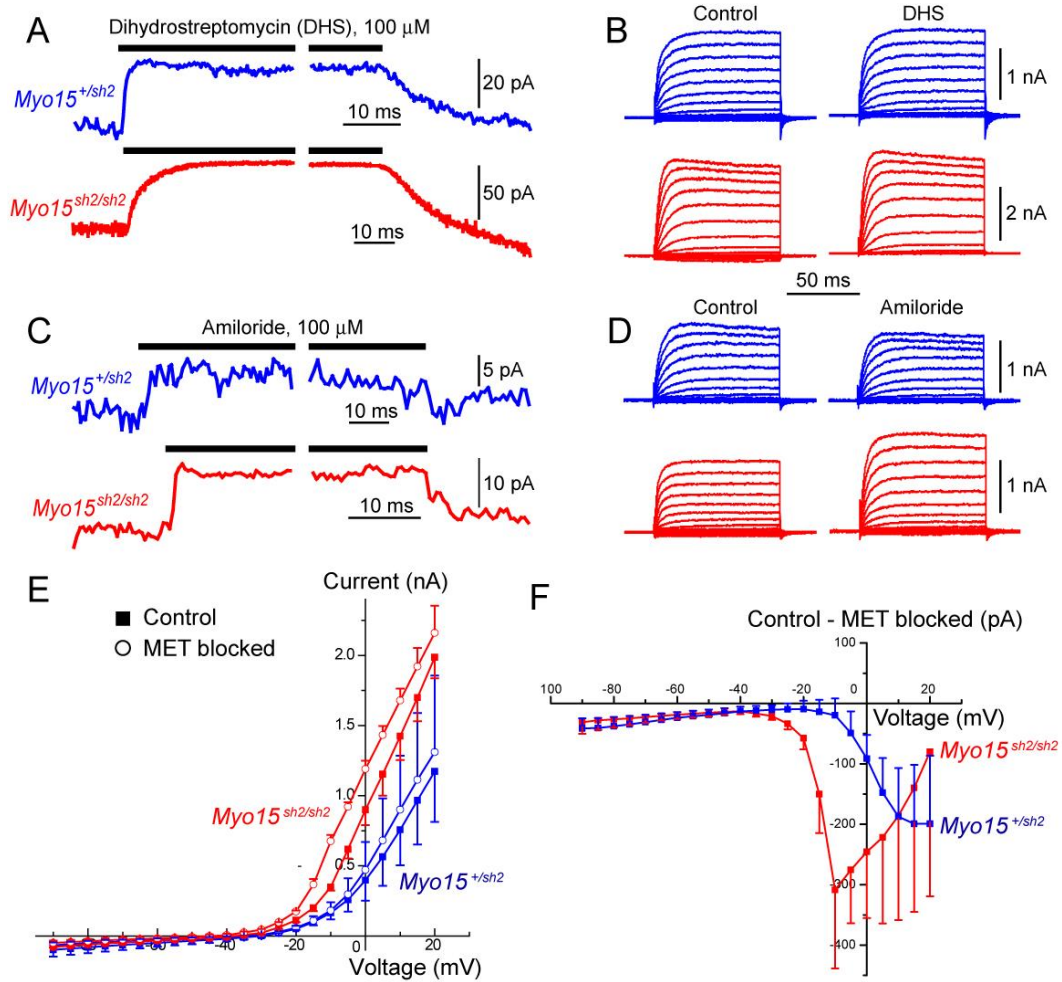


Figure 5.4-1: Effect of drugs blocking MET current on OHC ionic conductance. DHS (A) and Amiloride (C) reduce the inward current at holding potential of -60 mV in both *Myo15*^{+/sh2} (blue) and *Myo15*^{sh2/sh2} (red) OHCs. Voltage-step protocols also revealed similar effects of DHS (B) and Amiloride (D) on voltage-gated ionic conductance in *Myo15*^{+/sh2} and *Myo15*^{sh2/sh2} OHCs. (E) Combined I-V curves showing the effect of MET channel blocking on ionic currents. (F) Subtraction of the whole cell current after MET channel blocking from the control current shows that there is a MET-dependent inward current at negative potentials in both *Myo15*^{+/sh2} and *Myo15*^{sh2/sh2} OHCs, while larger MET-dependent outward current in *Myo15*^{sh2/sh2} OHCs. Number of cells: n=6 (*Myo15*^{+/sh2}), n=11 (*Myo15*^{sh2/sh2}). Age of the cells: P3-5 + 1-5 div.

Because both drugs produced similar effects, its combined effect on the whole cell current is summarized in the I-V curves on panel E. The curves show that at its the negative potentials, the drugs block the constitutively open component of the MET current in both *Myo15*^{+/sh2} (blue) and *Myo15*^{sh2/sh2} (red) OHCs, as seen by reduction in the whole cell current. At the positive potentials, however, an increase of an outward current is observed in *Myo15*^{sh2/sh2} OHCs, while similar increase in *Myo15*^{+/sh2} OHCs was not yet statistically significant. Subtraction of the whole cell currents with blocked MET channels from the control currents revealed an identical MET-dependent contribution in *Myo15*^{+/sh2} and *Myo15*^{sh2/sh2} OHCs at negative potentials and a larger effect of MET blocking at positive potentials in *Myo15*^{sh2/sh2} OHCs (Figure 5.4-1, E). These changes in outward (presumably K⁺) conductance are also consistent with the changes of the reversal potential after blocking of the MET channels (Figure 5.4-2).

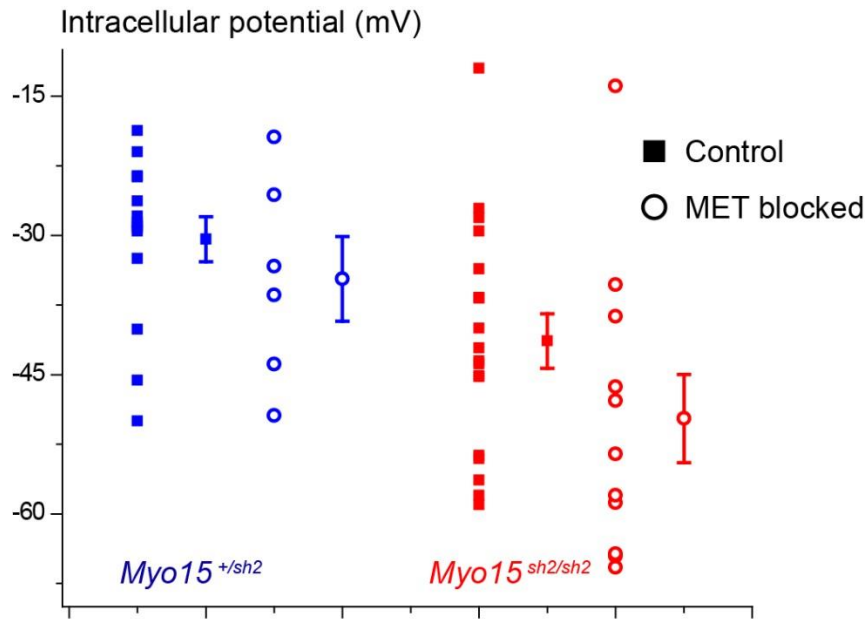


Figure 5.4-2: Reversal potential (V_{rev}) in *Myo15*^{+/sh2} (blue) and *Myo15*^{sh2/sh2} (red) OHCs without (solid square) or with (open circles) blocking of the MET channels.

V_{rev} is more negative in mutant cells under both conditions. The effect of MET blocking is more prominent in mutant OHCs.

Chapter 6 Summary

Deafness is a disability with high prevalence in the USA and around the world because of the many genes that are involved in the sense of hearing. As discussed in the first section of chapter three, genetic hearing loss can be caused because of damage to the hair cells or to the auditory nerve. Management of deafness is possible either by hearing aids or cochlear implant. Current research is focused on using Human embryonic stem-cells to regenerate the terminally differentiated hair cells and auditory nerve.

In the following section of the same chapter, the anatomy and function of the mammalian ear, cochlea and organ of Corti was covered. The organ of Corti has tonotopic property due to changes in the dimensions of the basilar membrane and in length of outer hair cells along the cochlea and so high frequency wavelength can be sensed at the base of cochlea while low frequencies are sensed at the apex. Comparisons between the inner and outer hair cells show that each cell's structure and enervation are compatible with its unique function despite their similarity in many aspects, like stereocilia linked with tensioned tip links which gate a Mechanotransduction (MET) channels at the tips of the stereocilia. The structure and function of stereocilia was described and their role in transduction current was elucidated.

Myosin15a was discussed in section 3.3. It is part of a large family of proteins and has many of the conserved functional domains. It is located at the tips of stereocilia and its function is to maintain the normal, staircase structure of stereocilia by interacting with the stereocilia's actin core and with other proteins in both inner and outer hair cells. Absence of Myosin15a due to a missense mutation in its motor domain results in abnormally short stereocilia in both hair cells and in degeneration and loss of tip links of the outer hair cells only. This mutation is linked to the genetic deafness DFNB3 and the *Shaker-2* (*Myo15a*^{sh/sh}) mouse model.

The original goal of this study was to investigate the existence of a potential “standing

current” in *Myo15^{sh2/sh2}* OHCs as a result of altered mechanical forces applied by the degenerating stereocilia on the MET channel. The used methods were described in chapter four. The process of cochlear dissection, on-the-spot genotyping, counting stereocilia and tip links, labeling hair cells by brief application of the dye FM1-43FX and Whole-cell patch clamp were explained.

Results were discussed in chapter five. Quantitative measurement of tip link per stereocilium shows stereocilia links rapidly deteriorate with age in *Myo15^{sh2/sh2}*. The decrease is very dramatic and is well below the normal number in wildtype cells. FM1-43FX dye uptake in old *Myo15^{sh2/sh2}* OHC who lost their tip links indicates the presence of constitutively open non-selective cation channels. Whole-cell patch clamp recordings were used in young explants OHCs to investigate the ionic conductances at resting, steady-state conditions in both *Myo15^{+/sh2}* and *Myo15^{sh2/sh2}*. Results show that there is a significant increase in outward current in *Myo15^{sh2/sh2}* OHCs ($p < 0.0566$) and a more negative intracellular potential ($p < 0.0206$). Blocking of the MET channels with Dihydrostreptomycin (DHS) and Amiloride, known blockers of the channel, reveals the existence of a standing inward current in both genotypes, an increase in the outward conductance of presumably K^+ current in *Myo15^{sh2/sh2}* and potential Ca^{2+} modulation of voltage-gated outward current.

Chapter 7 Conclusion

Examination of the scanning electron microscopy (SEM) images of *Myo15^{sh2/sh2}* OHCs revealed dramatic degeneration of stereocilia links after postnatal day 3 (P3). Despite this degeneration, we observed fast intracellular accumulation of FM1-43FX, a small cationic dye that is known to permeate through the MET channels, indicating that the MET channels are still open at rest in *Myo15^{sh2/sh2}* OHCs. A standing current that continuously flows into the cell through MET channels may result in a continuous influx of calcium leading to cell degeneration. Indeed, whole cell patch-clamp recordings revealed significant MET channel-dependent component of the ionic current in *Myo15^{sh2/sh2}* OHCs that was blocked by either dihydrostreptomycin (DHS) or Amiloride, known blockers of the MET channels. Thus, *Myo15^{sh2/sh2}* OHCs are likely to face an increased Ca^{2+} influx to the cell body due a decreased Ca^{2+} extrusion via stereociliar PMCA pumps (Figure 7-1), which may cause compensatory expression of additional voltage-gated K^+ channels to maintain intracellular potential and development of Ca^{2+} -dependent modulation of K^+ -conductance. This compensatory K^+ conductance(s) may explain a surprising increase of voltage-gated outward conductance in *Myo15^{sh2/sh2}* OHCs, which is further increased upon blocking of the MET channels. To the best of our knowledge, it is the first time that myosin 15a-deficiency has been associated with alterations of voltage-gated ion conductances.

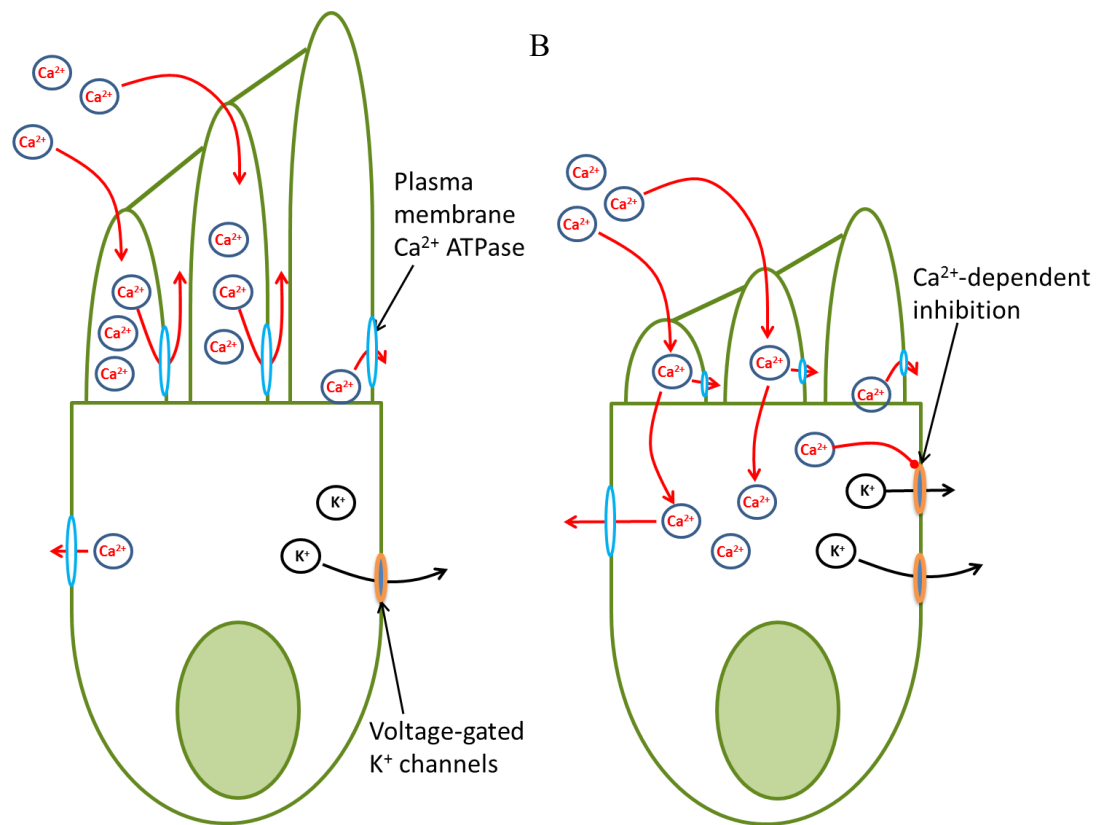


Figure 7-1: “Standing current” through partially open MET channels at rest are likely to produce different functional outcome in *Myo15*^{+/sh2} (left) and *Myo15*^{sh2/sh2} (right) OHCs. The Ca²⁺ entering through the MET channels in the normal *Myo15*^{+/sh2} OHCs is likely to be extruded by the very efficient stereocilia PMCA pumps, effectively shielding the soma of the cell from Ca²⁺. However, abnormally short stereocilia of *Myo15*^{sh2/sh2} OHCs have significantly smaller membrane area and hence less efficient Ca²⁺ extrusion. This may result in compensatory overexpression of voltage-gated K⁺ channel to maintain intracellular potential and development of Ca²⁺-dependent mechanisms of K⁺ channel modulation.

Appendix A

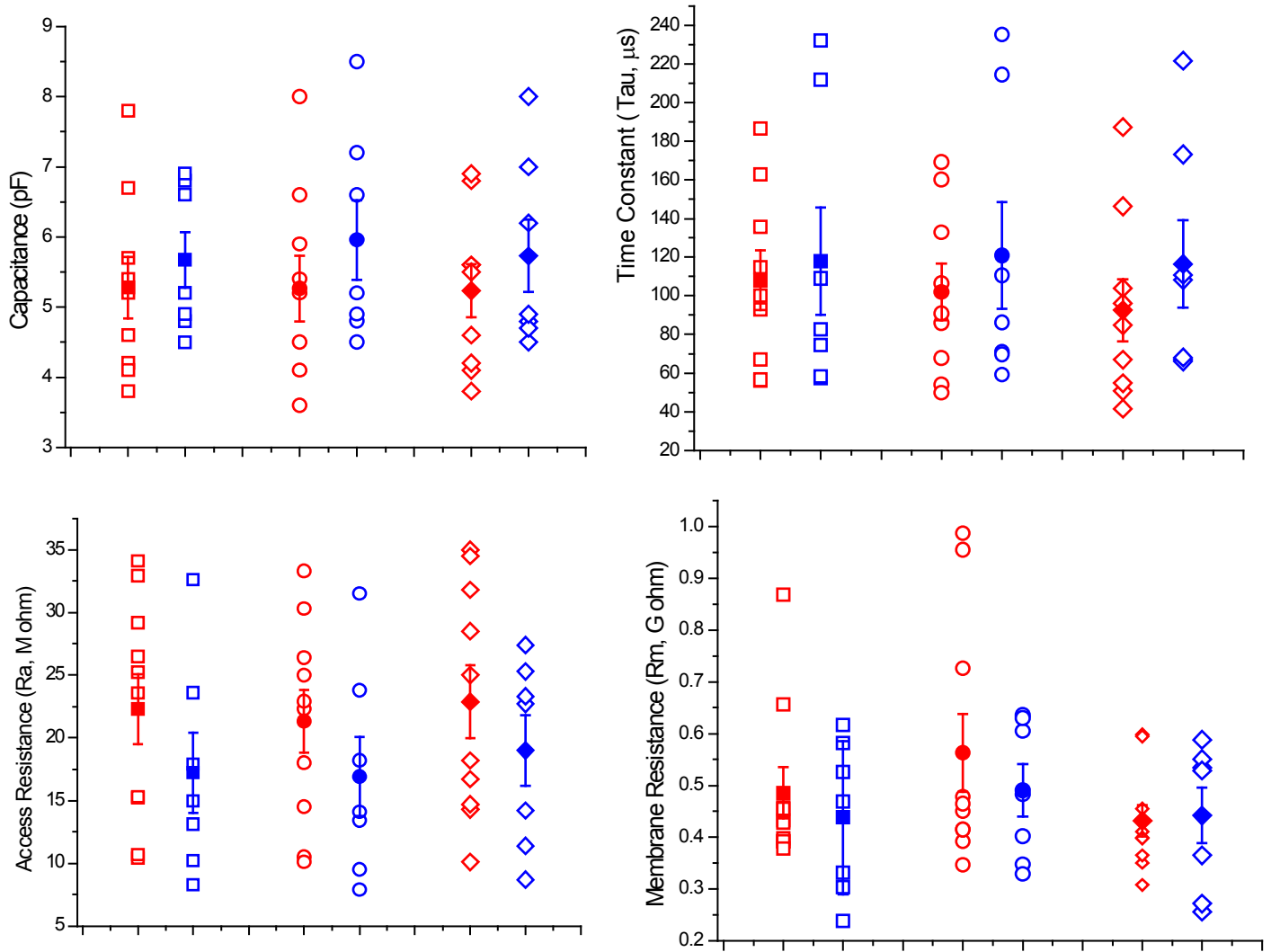


Figure A: Cell parameters in *Myo15*^{+/sh2} (blue) and *Myo15*^{sh2/sh2} (red) OHCs without (square) or with (circles) blocking of the MET channels and after blocker washout (diamond). Capacitance is indicative of cell's volume. The time constant of the membrane (Tau) represents the membrane's response to a step voltage. Access resistance (Ra) and membrane resistance (Rm) are indicative of seal quality. There is no significant change in parameters between the two genotypes in the presence or absence of blockers.

References

1. National Institute on Deafness and other Communication Disorders.
<http://www.nidcd.nih.gov/health/statistics/Pages/quick.aspx>. [Online] 2010.
2. "A gene for congenital, recessive deafness DFNB3 maps to the pericentromeric region of chromosome 17." . **Friedman, Thomas B., et al.** 1, (1995), Nature genetics, Vol. 9, pp. 86-91.
3. "Myosin XVa localizes to the tips of inner ear sensory cell stereocilia and is essential for staircase formation of the hair bundle." . **Belyantseva, Inna A., Erich T. Boger, and Thomas B. Friedman.** 24, (2003), Proceedings of the National Academy of Sciences, Vol. 100, pp. 13958-13963.
4. "Genetic Mapping Refines DFNB3 to 17p11. 2, Suggests Multiple Alleles of DFNB3, and Supports Homology to the Mouse Model shaker-2." . **Liang, Yong, et al.** 4, (1998), The American Journal of Human Genetics, Vol. 62, pp. 904-915.
5. "Auditory mechanotransduction in the absence of functional myosin-XVa." . **Stepanyan, Ruben, et al.** 3, (2006), The Journal of physiology , Vol. 576, pp. 801-808.
6. "Correction of deafness in shaker-2 mice by an unconventional myosin in a BAC transgene." . **Probst, Frank J., et al.** 5368, (1998), Science, Vol. 280, pp. 1444-1447.
7. "Gating properties of the mechano-electrical transducer channel in the dissociated vestibular hair cell of the chick." . **Ohmori, H. A. R. U. N. O. R. I.** 1, (1987), The Journal of physiology, Vol. 387, pp. 589-609.
8. "The actions of calcium on the mechano-electrical transducer current of turtle hair cells." . **Crawford, Andrew C., Michael G. Evans, and Robert Fettiplace.** 1, (1991), The Journal of physiology, Vol. 434, pp. 369-398.
9. "Ionic basis of the receptor potential in a vertebrate hair cell." . **Corey, D. P., and A. J. Hudspeth.** 5733, (1979), Nature , Vol. 281, p. 675.
10. "Mechano-electrical transduction currents in isolated vestibular hair cells of the chick." . **Ohmori, H. A. R. U. N. O. R. I.** 1, (1985), The Journal of physiology , Vol. 359, pp. 189-217.
11. "Detection of Ca²⁺ entry through mechanosensitive channels localizes the site of

- mechanoelectrical transduction in hair cells.*" . **Lumpkin, Ellen A., and A. J. Hudspeth.** 22, (1995), Proceedings of the National Academy of Sciences , Vol. 92, pp. 10297-10301.
12. *"Calcium permeation of the turtle hair cell mechanotransducer channel and its relation to the composition of endolymph."* . **Ricci, A. J., and R. Fettiplace.** 1, (1998), The Journal of physiology, Vol. 506, pp. 159-173.
13. *"Structural cell biology: Rapid renewal of auditory hair bundles."* . **Schneider, Mark E., et al.** 6900, (2002), Nature , Vol. 418, pp. 837-838.
14. National Institute on Deafness and other Communication Disorders. [Online] [Cited: 2 17, 2014.] <http://www.nidcd.nih.gov/health/statistics/Pages/quick.aspx>.
15. *"Restoration of auditory evoked responses by human ES-cell-derived otic progenitors."* . **Chen, Wei, et al.** (2012), Nature , Vol. 490.7419, pp. 278-282.
16. Ear Antomy. *WikiMedia*. [Online] [Cited: 2 17, 2014.] http://commons.wikimedia.org/wiki/File:Blausen_0328_EarAnatomy.png.
17. Pinna_(anatomy). *Wikipedia*. [Online] [Cited: 2 5, 2014.] http://en.wikipedia.org/wiki/Pinna_%28anatomy%29.
18. cochlea. *WikiMedia commons*. [Online] [Cited: 03 22, 2014.] http://commons.wikimedia.org/wiki/File:1406_Cochlea.jpg.
19. *Element composition of inner ear lymphs in cats, lizards, and skates determined by electron probe microanalysis of liquid samples.* **Scott K. Peterson, Lawrence S. Frishkopff, Claude Lechène, Charles M. Oman, Thomas F. Weiss.** 1, 1978, Journal of Comparative Physiology, Vol. 126.
20. *"Hair cells—beyond the transducer."* . **Housley, G. D., et al.** (2006), The Journal of membrane biology, Vols. 209.2-3, pp. 89-118.
21. *"Prestin is the motor protein of cochlear outer hair cells."* . **Zheng, Jing, et al.** 6783 , 2000, Nature , Vol. 405, pp. 149-155.
22. *Isolation of a novel PDZ-containing myosin from hematopoietic supportive bone marrow stromal cell lines.* **Furusawa T, Ikawa S, Yanai N, Obinata M.** 2000, Biochem Biophys Res Commun, Vol. 270, pp. 67-75.
23. *"Myosins: a diverse superfamily."* . **Sellers, James R.** 1, (2000), Biochimica et Biophysica Acta (BBA)-Molecular Cell Research, Vol. 1496, pp. 3-22.

24. *"The 95F unconventional myosin is required for proper organization of the Drosophila syncytial blastoderm."* **Mermall, Valerie, and Kathryn G. Miller.** 6, (1995), The Journal of cell biology , Vol. 129, pp. 1575-1588.
25. *"Myosin XVa."* **Boger, Erich T., et al.** 2008., Myosins. Springer Netherlands, pp. 441-467.
26. *"Myosin XVa and whirlin, two deafness gene products required for hair bundle growth, are located at the stereocilia tips and interact directly."* **Delprat, Benjamin, et al.** 3, (2005), Human molecular genetics , Vol. 14, pp. 401-410.
27. *"Regulation of stereocilia length by myosin XVa and whirlin depends on the actin-regulatory protein Eps8."* **Manor, Uri, et al.** 2, (2011), Current Biology , Vol. 21, pp. 167-172.
28. *"Evidence for opening of hair-cell transducer channels after tip-link loss."* **Meyer, Jens, et al.** 17, (1998), The Journal of neuroscience, Vol. 18, pp. 6748-6756.
29. *A quantitative comparison of mechanoelectrical transduction in vestibular and auditory hair cells of neonatal mice.* **Geleoc GS, Lennan GW, Richardson GP & Kros CJ.** (1997), Proc R Soc Lond B Biol Sci, Vol. 264, pp. 611–621.
30. *Tonotopic variation in the conductance of the hair cell mechanotransducer channel.* **Ricci AJ, Crawford AC & Fettiplace R.** (2003), Neuron, Vol. 40, pp. 983-990.
31. *"Usher proteins in inner ear structure and function."* **Ahmed, Zubair M., Gregory I. Frolenkov, and Saima Riazuddin.** 21, (2013), Physiological genomics, Vol. 45 , pp. 987-989.
32. *"Block by amiloride and its derivatives of mechano-electrical transduction in outer hair cells of mouse cochlear cultures."* **Rüsch, A., C. J. Kros, and G. P. Richardson.** 1, (1994), The Journal of Physiology, Vol. 474, pp. 75-86.
33. *"Mechano-electrical transducer currents in hair cells of the cultured neonatal mouse cochlea."* **Kros, C. J., A. Rusch, and G. P. Richardson.** 1325, (1992), Proceedings of the Royal Society of London. Series B: Biological Sciences , Vol. 249, pp. 185-193.
34. *"Aminoglycoside antibiotics."* **Forge, Andrew, and Jochen Schacht.** 1, (2000), Audiology and Neurotology, Vol. 5, pp. 3-22.
35. *"Blockage of the transduction channels of hair cells in the bullfrog's sacculus by aminoglycoside antibiotics."* **Kroese, A. B. A., A. Das, and A. J. Hudspeth.** 3, (1989),

Hearing research , Vol. 37, pp. 203-217.

36. "Human Nonsyndromic Sensorineural Deafness." . **Friedman, Thomas B., and Andrew J. Griffith.** 1, 2003, Annual review of genomics and human genetics, Vol. 4, pp. 341-402.

37. "A Novel Type of Myosin Encoded by the Mouse Deafness Gene *shaker-2*." . **Wakabayashi, Y., et al.** 3, (1998), Biochemical and biophysical research communications, Vol. 248, pp. 655-659.

38. Kata Kolok. *Wikipedia*. [Online] [Cited: 21, 2014.]
http://en.wikipedia.org/wiki/Kata_Kolok.

39. Association of Unconventional Myosin MYO15 mutations with human non-syndromic deafness DFNB3. **Wang.** 1998, Science 280.

40. "Characterization of the Human and Mouse Unconventional Myosin XV Genes Responsible for Hereditary Deafness DFNB3 and Shaker 2." . **Liang, Yong, et al.** 3, (1999), Genomics, Vol. 61, pp. 243-258.

41. A physical map of the mouse shaker-2 region contains many of the genes commonly deleted in Smith-Magenis syndrome (del17p11.2p11.2). **Probst F. J., Chen K. S., Zhao Q., Wang A., Friedman T. B., Lupski J. R., and Camper S. A.** (1999), Genomics, Vol. 55, pp. 348–52.

42. **Belyantseva, Inna A.** "Helios® Gene Gun–Mediated Transfection of the Inner Ear Sensory Epithelium." . *Auditory and Vestibular Research*. s.l. : Humana Press, 2009. , pp. 103-124.

43. Cochlea image. *WIKIMEDIA COMMONS*. [Online] [Cited: Jan 16, 2014.]
<http://commons.wikimedia.org/wiki/File:Cochl%C3%A9e.png>.

44. "Development and regeneration of sensory transduction in auditory hair cells requires functional interaction between cadherin-23 and protocadherin-15." . **Lelli, Andrea, et al.** 34, (2010), The Journal of Neuroscience, Vol. 30, pp. 11259-11269.

45. FM1-43 dye behaves as a permeant blocker of the hair-cell mechanotransducer channel. **Gale JE, Marcotti W, Kennedy HJ, Kros CJ & Richardson GP.** (2001), J Neurosci, Vol. 21, pp. 7013–7025.

46. MYO15A (DFNB3) mutations in Turkish hearing loss families and functional modeling of a novel motor domain mutation. **Kalay E, Uzumcu A, Krieger E, Cayan**

R, Uyguner O, Ulubil-Emiroglu M, Erdol H, Kayserili H, Hafiz G, Bas,erer N, Heister AJGM, Hennies HC, Nu"rnberg P, Bas,aran S, Brunner HG, Cremers CWRJ, Karaguzel A, Wollnik B, Kremer H. 2007., Am J Med Genet, pp. Part A 143A:2382–2389.

47. *"The motor and tail regions of myosin XV are critical for normal structure and function of auditory and vestibular hair cells."* . **Anderson, David W., et al.** 12, (2000), Human molecular genetics , Vol. 9, pp. 1729-1738.

48. *"What is the hair cell transduction channel?."* . **Corey, David P.** 1, (2006), The Journal of physiology, Vol. 576, pp. 23-28.

49. *"Probing the pore of the auditory hair cell mechanotransducer channel in turtle."* . **Farris, H. E., et al.** 3, (2004), The Journal of physiology, Vol. 558, pp. 769-792.

50. *"Age-related changes in cochlear gene expression in normal and shaker 2 mice."* . **Gong, Tzy-Wen L., et al.** 3, 2006, JARO-Journal of the Association for Research in Otolaryngology, Vol. 7, pp. 317-328.

51. *"Mechanisms of hair cell death and protection."* . **Cheng, Alan G., Lisa L. Cunningham, and Edwin W. Rubel.** 6, 2005, Current opinion in otolaryngology & head and neck surgery ., Vol. 13, pp. 343-348.

52. *"Mechanotransduction by hair cells: models, molecules, and mechanisms."* . **Gillespie, Peter G., and Ulrich Müller.** 1, (2009), Cell , Vol. 139, pp. 33-44.

53. *"Mouse models to study inner ear development and hereditary hearing loss."* . **Friedman, LILACH M., AMIEL A. Dror, and Karen B. Avraham.** (2007), International Journal of Developmental Biology, Vol. 51.6/7, pp. 609-631.

54. *"A cytoskeletal spring in cochlear outer hair cells."* . **Holley, M. C., and J. F. Ashmore.** 6191, (1988), Nature, Vol. 335, pp. 635-637.

55. *"Unconventional myosins in inner-ear sensory epithelia."* . **Hasson, Tama, et al.** 6, (1997), The Journal of cell biology, Vol. 137, pp. 1287-1307.

56. *"Mutations in the first MyTH4 domain of MYO15A are a common cause of DFNB3 hearing loss."* . **Shearer, A. Eliot, et al.** 4, (2009), The Laryngoscope , Vol. 119, pp. 727-733.

57. *"Myosin function in nervous and sensory systems."* . **Brown, Michael E., and Paul C. Bridgman.** 1, (2004), Journal of neurobiology , Vol. 58, pp. 118-130.

58. *"Myosin motor function: the ins and outs of actin-based membrane protrusions."*. **Nambiar, Rajalakshmi, Russell E. McConnell, and Matthew J. Tyska.** 8, (2010), Cellular and molecular life sciences, Vol. 67, pp. 1239-1254.
59. *"Myo15 function is distinct from Myo6, Myo7a and pirouette genes in development of cochlear stereocilia."*. **Karolyi, I. Jill, et al.** 21, (2003), Human molecular genetics, Vol. 12, pp. 2797-2805.
60. *"Auditory transduction in the mouse."*. **Grant, Lisa, and Paul A. Fuchs.** 5, (2007), Pflügers Archiv-European Journal of Physiology, Vol. 454, pp. 793-804.
61. *"Sensory transduction and adaptation in inner and outer hair cells of the mouse auditory system."*. **Stauffer, Eric A., and Jeffrey R. Holt.** 6, (2007), Journal of neurophysiology, Vol. 98, pp. 3360-3369.
62. *"Tonotopic gradient in the developmental acquisition of sensory transduction in outer hair cells of the mouse cochlea."*. **Lelli, Andrea, et al.** 6, (2009), Journal of neurophysiology, Vol. 101, pp. 2961-2973.
63. *"Hair cells in the inner ear of the pirouette and shaker 2 mutant mice."*. **Beyer, Lisa A., et al.** 4, (2000), Journal of neurocytology, Vol. 29, pp. 227-240.
64. *"Protection against noise-induced hearing loss in young CBA/J mice by low-dose kanamycin."*. **Fernandez, Elizabeth A., et al.** 2, (2010), Journal of the Association for Research in Otolaryngology, Vol. 11, pp. 235-244.
65. *"Functional hair cell mechanotransducer channels are required for aminoglycoside ototoxicity."*. **Alharazneh, Abdelrahman, et al.** 7, (2011), PLoS One, Vol. 6, p. e22347.
66. *"Nonsyndromic hearing impairment: unparalleled heterogeneity."*. **Van Camp, Guy, Patrick J. Willems, and R. J. Smith.** 4, (1997), American journal of human genetics, Vol. 60, p. 758.
67. *"Structure of the cortical cytoskeleton in mammalian outer hair cells."*. **Holley, M. C., F. Kalinec, and B. Kachar.** 3, (1992), Journal of cell science, Vol. 102, pp. 569-580.
68. *"The aminoglycoside antibiotic dihydrostreptomycin rapidly enters mouse outer hair cells through the mechano-electrical transducer channels."*. **Marcotti, Walter, Sietse M. Van Netten, and Corné J. Kros.** 2, (2005), The Journal of physiology, Vol. 567, pp. 505-521.
69. *"Defining features of the hair cell mechanoelectrical transducer channel."*.

- Fettiplace, Robert.** 6, (2009), Pflügers Archiv-European Journal of Physiology, Vol. 458, pp. 1115-1123.
70. "*Mechanotransduction in mouse inner ear hair cells requires transmembrane channel-like genes.*" . **Kawashima, Yoshiyuki, et al.** 12, (2011), The Journal of clinical investigation, Vol. 121, p. 4796.
71. "*Unconventional myosins and the genetics of hearing loss.*". **Friedman, Thomas B., James R. Sellers, and Karen B. Avraham.** 3, (1999), American journal of medical genetics, Vol. 89, pp. 147-157.
72. "*The micromachinery of mechanotransduction in hair cells.*". **Vollrath, Melissa A., Kelvin Y. Kwan, and David P. Corey.** (2007), Annual review of neuroscience, Vol. 30, p. 339.
73. "*Localization of the hair cell's transduction channels at the hair bundle's top by iontophoretic application of a channel blocker.*". **Jaramillo, Fernán, and A. J. Hudspeth.** 3, (1991), Neuron, Vol. 7, pp. 409-420.
74. "*Fate of mammalian cochlear hair cells and stereocilia after loss of the stereocilia.*" . **Jia, Shuping, et al.** 48, (2009), The Journal of Neuroscience , Vol. 29, pp. 15277-15285.
75. "*Myosin-XVa is required for tip localization of whirlin and differential elongation of hair-cell stereocilia.*". **Belyantseva, Inna A., et al.** 2, (2005), Nature cell biology, Vol. 7, pp. 148-156.
76. "*Mechanotransduction by hair cells: models, molecules, and mechanisms.*". **Gillespie, Peter G., and Ulrich Müller.** 1, (2009), Cell , Vol. 139, pp. 33-44.
77. "*Probing the pore of the auditory hair cell mechanotransducer channel in turtle.*". **Farris, H. E., et al.** 3, (2004), The Journal of physiology, Vol. 558, pp. 769-792.
78. "*The sensory and motor roles of auditory hair cells.*" . **Fettiplace, Robert, and Carole M. Hackney.** 1, (2006), Nature Reviews Neuroscience , Vol. 7, pp. 19-29.
79. "*Development of the hair bundle and mechanotransduction.*". **Nayak, Gowri D., et al.** 6/7, (2007), International journal of developmental biology , Vol. 51, p. 597.
80. "*Differences in mechano-transducer channel kinetics underlie tonotopic distribution of fast adaptation in auditory hair cells.*". **Ricci, Anthony.** 4, (2002), Journal of neurophysiology, Vol. 87, pp. 1738-1748.
81. "*Tip links in hair cells: molecular composition and role in hearing loss.*". **Sakaguchi,**

- Hirofumi, et al.** 5, (2009), Current opinion in otolaryngology & head and neck surgery, Vol. 17, p. 388.
82. *"The mechanotransduction machinery of hair cells."* **Grillet, Nicolas, et al.** 85, (2009), Science signaling, Vol. 2, p. pt5.
83. *"Mechanotransduction: all signals point to cytoskeleton, matrix, and integrins."* **Alenghat, Francis J., and Donald E. Ingber.** 119, (2002), Science Signaling , Vol. 2002, p. pe6.
84. *"A Drosophila mechanosensory transduction channel."* **Walker, Richard G., Aaron T. Willingham, and Charles S. Zuker.** 5461, (2000), Science Signaling, Vol. 287, p. 2229.
85. *"The selectivity of the hair cell's mechanoelectrical-transduction channel promotes Ca^{2+} flux at low Ca^{2+} concentrations."* **Lumpkin, Ellen A., Robert E. Marquis, and A. J. Hudspeth.** 20, (1997), Proceedings of the National Academy of Sciences, Vol. 94, pp. 10997-11002.
86. *"Mechanosensitive channel properties and membrane mechanics in mouse dystrophic myotubes."* **Suchyna, Thomas M., and Frederick Sachs.** 1, (2007), The Journal of physiology, Vol. 581, pp. 369-387.
87. *"Effects of stretch-activated channel blockers on $[Ca^{2+}]_i$ and muscle damage in the mdx mouse."* **Yeung, Ella W., et al.** 2, The Journal of physiology , Vol. 562, pp. 367-380.
88. *"Dihydrostreptomycin modifies adaptation and blocks the mechano-electric transducer in chick cochlear hair cells."* **Kimitsuki, Takashi, and Harunori Ohmori.** 1, (1993), Brain research, Vol. 624, pp. 143-150.
89. *"Kinetics of the receptor current in bullfrog saccular hair cells."* **Corey, D. P., and A. J. Hudspeth.** 5, (1983), The Journal of Neuroscience , Vol. 3, pp. 962-976.
90. *"Correction of deafness in shaker-2 mice by an unconventional myosin in a BAC transgene."* **Probst, Frank J., et al.** 5368, (1998), Science, Vol. 280, pp. 1444-1447.
91. *"Novel mutations of MYO15A associated with profound deafness in consanguineous families and moderately severe hearing loss in a patient with Smith-Magenis syndrome."* **Liburd, Nikki, et al.** 5, (2001), Human genetics , Vol. 109, pp. 535-541.
92. *"Myosin superfamily evolutionary history."* **Thompson, Reid F., and George M.**

- Langford.** 3, (2002), *The Anatomical Record*, Vol. 268, pp. 276-289.
93. "An actin molecular treadmill and myosins maintain stereocilia functional architecture and self-renewal." . **Rzadzinska, Agnieszka K., et al.** 6, (2004), *The Journal of cell biology*, Vol. 164, pp. 887-897.
94. *Lighting up the senses: FM1-43 loading of sensory cells through nonselective ion channels.* **Meyers JR, Macdonald RB, Duggan A, Lenzi D, Standaert DG, Corwin JT & Corey DP.** (2003), *J Neurosci* , Vol. 23, pp. 4054–4065.
95. *TRPA1 is a candidate for the mechanosensitive transduction channel of vertebrate hair cells.* **Corey, D.P., Garcia-Anoveros, J., Holt, J.R., Kwan, K.Y., Lin, S.Y., Vollrath, M.A., Amalfitano, A., Cheung, E.L., Derfler, B.H., Duggan, A., et al.** (2004), *Nature*, Vol. 432, pp. 723–730.
96. "Sisyphus, the *Drosophila* myosin XV homolog, traffics within filopodia transporting key sensory and adhesion cargos." . **Liu, Raymond, et al.** 1, 2008, *Development*, Vol. 135, pp. 53-63.
97. **WIKIMEDIA COMMONS.** Structure of Amiloride. [Online] [Cited: Jan 5, 2014.] http://commons.wikimedia.org/wiki/File:Amilorid_-_Amiloride.svg.
98. **WIKIMEDIA COMMONS.** chemical structure of Dihydrostreptomycin. [Online] [Cited: Jan 5, 2014.] <http://commons.wikimedia.org/wiki/File:Dihydrostreptomycin.png#>.
99. **Jackson, M. B.** Whole-Cell Voltage Clamp Recording. . *Current Protocols in Neuroscience*. 2001., pp. 6.6.1–6.6.30.
100. **Molleman, Areles.** *Front Matter, in Patch Clamping: An Introductory Guide To Patch Clamp Electrophysiology.* s.l. : John Wiley & Sons, Ltd., 2003.
101. *DFNB3 families and Shaker-2 mice: mutations in an unconventional myosin, myo 15.* **Friedman TB, Hinnant JT, Fridell RA, Wilcox ER, Raphael Y, Camper SA.** 2000, *Advances in Oto-Rhino-Laryngology*.
102. "Extracellular matrices associated with the apical surfaces of sensory epithelia in the inner ear: molecular and structural diversity." . **Goodyear, Richard J., and Guy P. Richardson.** 2, (2002), *Journal of neurobiology*, Vol. 53, pp. 212-227.
103. "Fast adaptation and Ca²⁺ sensitivity of the mechanotransducer require myosin-XVa in inner but not outer cochlear hair cells." . **Stepanyan, Ruben, and Gregory I. Frolenkov.** 13, 2009, *The Journal of Neuroscience*, Vol. 29, pp. 4023-4034.

104. *Differential vulnerability of basal and apical hair cells is based on intrinsic susceptibility to free radicals.* **Sha SH, Taylor R, Forge A, Schacht J.** 2001, Hearing Res, Vol. 155, pp. 1-8.
105. *"Plasma membrane Ca^{2+} -ATPase isoform 2a is the PMCA of hair bundles."* .
Dumont, Rachel A., et al. 14, 2001, The Journal of Neuroscience, Vol. 21, pp. 5066-5078.

Vita

Diana F. Syam

EDUCATION

University of Jordan, Amman, Jordan
B.Sc. in Medical Technology **2011**

PROFESSIONAL EXPERIENCE

Physiology Laboratory, University of Kentucky
Researcher **2012-2014**

Molecular Pharmacology Laboratory, University of Kentucky
Researcher **2012**

Medical Microbiology Laboratory, University of Jordan, Jordan
Researcher **2010**

PUBLICATIONS

- D. Syam et al., "Immobilizing mutation in an unconventional myosin15a affects not only the structure of mechanosensory stereocilia in the inner ear hair cells but also their ionic conductances" *In Preparation*
- D. Syam et al., "Does Myosin-XVa deficiency result in constitutively open mechanotransduction channel", poster at the first meeting for Kentucky Physiological Society 2012-2013.
- D. Syam et al., "Degeneration of cochlear outer hair cells in the mouse model of non-syndromic deafness,DFNB3", poster at the 8th Annual Spring Conference hosted by UK Center for Clinical and Translational Science 2013.